

file

PROGRESS REPORT

ON

**CORRELATION OF LABORATORY TESTS WITH
FULL SCALE SHIP PLATE FRACTURE TESTS:
A STUDY OF STRAIN GRADIENTS**

BY

**E. P. KLIER, F. C. WAGNER, J. L. FISHER
and M. GENSAMER**

**Pennsylvania State College
Under Bureau of Ships Contract NObs-31217**

COMMITTEE ON SHIP CONSTRUCTION

DIVISION OF ENGINEERING AND INDUSTRIAL RESEARCH

NATIONAL RESEARCH COUNCIL

MTRB LIBRARY

ADVISORY TO

SHIP STRUCTURE COMMITTEE

UNDER

**Bureau of Ships, Navy Department
Contract NObs-34231**

SERIAL NO. SSC-17

COPY NO. 143

DATE: JUNE 8, 1949

NATIONAL RESEARCH COUNCIL
2101 CONSTITUTION AVENUE, WASHINGTON, D. C.

Established in 1916 by the National Academy of Sciences under its Congressional
Charter and organized with the cooperation of the National Scientific
and Technical Societies of the United States

DIVISION OF ENGINEERING AND INDUSTRIAL RESEARCH

June 8, 1949

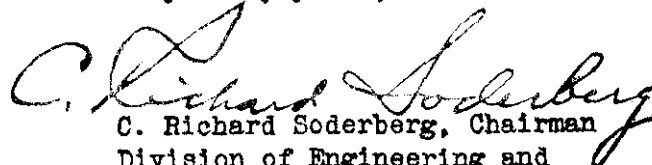
Chief, Bureau of Ships
Navy Department
Washington 25, D. C.

Dear Sir:

Attached is Report Serial No. SS-17, entitled
"Correlation of Laboratory Tests with Full Scale Ship Plate
Fracture Tests: A Study of Strain Gradients." This report
has been submitted by the contractor as a Progress Report of
the work done on Research Project SR-96 under Contract
NObs-31217 between the Bureau of Ships, Navy Department
and Pennsylvania State College.

The report has been reviewed and acceptance recom-
mended by representatives of the Committee on Ship Construction,
Division of Engineering and Industrial Research, NRC, in
accordance with the terms of the contract between the Bureau
of Ships, Navy Department and the National Academy of Sciences.

Very truly yours,


C. Richard Soderberg, Chairman
Division of Engineering and
Industrial Research

CRS:mh
Enclosure

PREFACE

The Navy Department through the Bureau of Ships is distributing this report to those agencies and individuals who were actively associated with the research work. This report represents a part of the research work contracted for under the section of the Navy's directive "to investigate the design and construction of welded steel merchant vessels."

The distribution of this report is as follows:

Copy No. 1 - Chief, Bureau of Ships, Navy Department
Copy No. 2 - Dr. D. W. Bronk, Chairman, National Research Council

Committee on Ship Construction

Copy No. 3 - V. H. Schnee, Chairman
Copy No. 4 - J. L. Bates
Copy No. 5 - H. C. Boardman
Copy No. 6 - Paul Ffield
Copy No. 7 - M. A. Grossman
Copy No. 8 - C. H. Herty, Jr.
Copy No. 9 - A. B. Kinzel
Copy No. 10 - J. M. Lessells
Copy No. 11 - G. S. Mikhalapov
Copy No. 12 - J. Ormondroyd
Copy No. 13 - H. W. Pierce
Copy No. 14 - E. C. Smith
Copy No. 15 - T. T. Watson
Copy No. 16 - Finn Jonassen, Research Coordinator

Members of Project Advisory Committees SR-25, SR-87, SR-92,
SR-96, SR-98, SR-99, SR-100 and SR-101

Copy No. 16 - Finn Jonassen, Chairman
Copy No. 17 - R. H. Aborn
Copy No. 18 - L. C. Bibber
Copy No. 5 - H. C. Boardman
Copy No. 19 - T. J. Dolan
Copy No. 6 - Paul Ffield
Copy No. 7 - M. A. Grossman
Copy No. 8 - C. H. Herty, Jr.
Copy No. 20 - C. E. Jackson
Copy No. 10 - J. M. Lessells
Copy No. 21 - M. W. Lightner
Copy No. 11 - G. S. Mikhalapov
Copy No. 12 - J. Ormondroyd
Copy No. 22 - R. E. Peterson
Copy No. 13 - H. W. Pierce
Copy No. 23 - R. L. Rickett
Copy No. 14 - E. C. Smith
Copy No. 15 - T. T. Watson
Copy No. 24 - A. G. Bissell, Bureau of Ships, Liaison
Copy No. 25 - Mathew Letich, American Bureau of Shipping, Liaison

*M. B. M. Wundt, General Electric Co; Schenectady, N.Y. 1 Copy
1/27/60*

- Copy No. 26 - James McIntosh, U. S. Coast Guard, Liaison
- Copy No. 27 - ~~E. Rassman, Bureau of Ships, Liaison~~ *Dr. Rivers - Stevens - 5/6/52*
- Copy No. 28 - Comdr. R. D. Schmidtman, U. S. Coast Guard, Liaison
- Copy No. 29 - T. L. Soo-Hoo, Bureau of Ships, Liaison
- Copy No. 30 - Wm. Spraragen, Welding Research Council, Liaison
- Copy No. 31 - R. E. Wiley, Bureau of Ships, Liaison
- Copy No. 32 - J. L. Wilson, American Bureau of Shipping, Liaison

Ship Structure Committee

- Copy No. 33 - Rear Admiral Ellis Reed-Hill, USCG - Chairman
- Copy No. 34 - Rear Admiral Charles D. Wheelock, USN, Bureau of Ships
- Copy No. 35 - Brigadier General Paul F. Yount, War Department
- Copy No. 36 - Captain J. L. McGuigan, U. S. Maritime Commission
- Copy No. 37 - D. P. Brown, American Bureau of Shipping
- Copy No. 3 - V. H. Schnee, Committee on Ship Construction - Liaison

Ship Structure Subcommittee

- Copy No. 38 - Captain C. M. Tooke, USN, Bureau of Ships, Chairman
- Copy No. 39 - Captain R. A. Hinners, USN, David Taylor Model Basin
- Copy No. 40 - Comdr. R. H. Lambert, USN, Bureau of Ships
- Copy No. 28 - Comdr. R. D. Schmidtman, USCG, U.S. Coast Guard Headquarters
- Copy No. 41 - W. G. Frederick, U. S. Maritime Commission
- Copy No. 42 - Hubert Kempel, Office, Chief of Transportation, War Department
- Copy No. 25 - Mathew Letich, American Bureau of Shipping
- Copy No. 26 - James McIntosh, U. S. Coast Guard
- Copy No. 43 - R. M. Robertson, Office, Naval Research, U. S. Navy
- Copy No. 44 - V. L. Russo, U. S. Maritime Commission
- Copy No. 31 - R. E. Wiley, Bureau of Ships, U. S. Navy
- Copy No. 32 - J. L. Wilson, American Bureau of Shipping
- Copy No. 16 - Finn Jonassen, Liaison Representative, NRC
- Copy No. 45 - E. H. Davidson, Liaison Representative, AISI
- Copy No. 46 - Paul Gerhart, Liaison Representative, AISI
- Copy No. 30 - Wm. Spraragen, Liaison Representative, WRC

Navy Department

- Copy No. 47 - Comdr. R. S. Mandelkorn, USN, Armed Forces Special Weapons Project
- Copy No. 24 - A. G. Bissell, Bureau of Ships
- Copy No. 48 - A. Amirikian, Bureau of Yards and Docks
- Copy No. 49 - J. W. Jenkins, Bureau of Ships
- Copy No. 50 - Noah Kahn, New York Naval Shipyard
- Copy No. 51 - E. M. MacCutcheon, Jr., David Taylor Model Basin
- Copy No. 52 - W. R. Osgood, David Taylor Model Basin
- Copy No. 53 - N. E. Promisel, Bureau of Aeronautics
- Copy No. 54 - John Vasta, Bureau of Ships
- Copies 55 and 56 - U. S. Naval Engineering Experiment Station
- Copy No. 57 - New York Naval Shipyard, Material Laboratory
- Copy No. 58 - Industrial Testing Laboratory, Philadelphia Naval Shipyard
- Copy No. 59 - Philadelphia Naval Shipyard
- Copy No. 60 - San Francisco Naval Shipyard

Copy No. 61 - David Taylor Model Basin, Attn: Library
Copies 62 and 63 - Publications Board, Navy Department via BuShips, Code 330c
Copies 64 and 65 - Technical Library, Bureau of Ships, Code 337-L

U. S. Coast Guard

Copy No. 66 - Captain R. B. Lank, Jr., USCG
Copy No. 67 - Captain G. A. Tyler, USCG
Copy No. 68 - Testing and Development Division
Copy No. 69 - U. S. Coast Guard Academy, New London

U. S. Maritime Commission

Copy No. 70 - E. E. Martinsky

Representatives of American Iron and Steel Institute
Committee on Manufacturing Problems

Copy No. 71 - C. M. Parker, Secretary, General Technical Committee,
American Iron and Steel Institute
Copy No. 18 - L. C. Bibber, Carnegie-Illinois Steel Corp.
Copy No. 8 - C. H. Herty, Jr., Bethlehem Steel Company
Copy No. 14 - E. C. Smith, Republic Steel Company

Welding Research Council

Copy No. 72 - C. A. Adams
Copy No. 73 - Everett Chapman
Copy No. 74 - LaMotte Grover
Copy No. 30 - Wm. Spraragen

Committee on Ship Steel

Copy No. 75 - P. F. Mehl, Chairman
Copy No. 8 - C. H. Herty, Jr., Vice Chairman
Copy No. 76 - Wm. M. Baldwin, Jr.
Copy No. 77 - Chas. S. Barrett
Copy No. 78 - R. M. Brick
Copy No. 79 - S. L. Hoyt
Copy No. 80 - I. R. Kramer
Copy No. 21 - M. W. Lightner
Copy No. 81 - T. S. Washburn
Copy No. 16 - Finn Jonassen, Technical Director
Copy No. 82 - R. H. Raring, Technical Secretary

Copy No. 83 - C. R. Soderberg, Chairman, Div. Eng. & Ind. Research, NRC
Copy No. 3 - V. H. Schnee, Chairman, Committee on Ship Construction
Copy No. 16 - Finn Jonassen, Research Coordinator, Committee on Ship Construction
Copy No. 84 - E. P. Klier, Investigator, Research Project SR-96
Copy No. 85 - F. C. Wagner, Investigator, Research Project SR-96
Copy No. 86 - J. L. Fisher, Investigator, Research Project SR-96
Copy No. 87 - M. Gensamer, Investigator, Research Project SR-96
Copy No. 88 - S. T. Carpenter, Investigator, Research Project SR-98
Copy No. 89 - L. J. Ebert, Investigator, Research Project SR-99
Copy No. 10 - J. M. Lessells, Investigator, Research Project SR-101

Copy No. 90 - C. W. MacGregor, Investigator, Research Project SR-102
 Copy No. 91 - C. B. Voldrich, Investigator, Research Project SR-100
 Copy No. 92 - Clarence Altenburger, Great Lakes Steel Company
 Copy No. 93 - A. B. Bagsar, Sun Oil Company
 Copy No. 94 - E. L. Cochrane, Massachusetts Institute of Technology
 Copy No. 95 - George Ellinger, National Bureau of Standards
 Copy No. 96 - M. F. Hawkes, Carnegie Institute of Technology
 Copy No. 97 - W. F. Hess, Rensselaer Polytechnic Institute
 Copy No. 98 - O. J. Horger, Timken Roller Bearing Company
 Copy No. 99 - Bruce Johnston, Fritz Laboratory, Lehigh University
 Copy No. 100 - P. E. Kyle, Cornell University
 Copy No. 101 - J. R. Low, Jr., General Electric Company
 Copy No. 102 - N. M. Newmark, University of Illinois
 Copy No. 103 - J. T. Norton, Massachusetts Institute of Technology
 Copy No. 104 - W. A. Reich, General Electric Company
 Copy No. 105 - L. J. Rohl, Carnegie-Illinois Steel Corp.
 Copy No. 106 - W. P. Roop, Swarthmore College
 Copy No. 107 - R. D. Stout, Lehigh University
 Copy No. 108 - Saylor Snyder, Carnegie-Illinois Steel Corp.
 Copy No. 109 - J. F. Wallace, Watertown Arsenal Laboratory (Staff)
 Copy No. 110 thru 134 - Sir Chas. Wright, British Joint Services Mission (Navy)
 Copy No. 135 - Carl A. Zapffe, Carl A. Zapffe Laboratories
 Copy No. 136 - International Nickel Co., Inc., Attn: T. N. Armstrong
 Copy No. 137 - Transportation Corps Board, Brooklyn, New York
 Copies 138 thru 142 - Library of Congress via Bureau of Ships, Code 330c
 Copy No. 143 - File Copy, Committee on Ship Steel
 Copy No. 144 - NACA, Attn: Materials Research Coordination, U. S. Navy
 Copies 145 thru 149 - Bureau of Ships

^{147-2-6. me. mat. - 2/6/50}
^{148-38-10-776. mechanics div. copy 3811 (4/17/51)}
 Copy No. 150 - *Critical Ship Welding Research Assn. Attn: J. C. Asher, Sec*
 Copy No. 151 - *Armour Research Foundation, at. Walter Craig, 7/1/51*
 Copy No. 152 - *H. Thomasson - Canadian Westinghouse Ltd. 5/8/51*
 Copy No. 153 - *Recd adm. H. C. Shepherd 2/11/52*
 Copy No. 154 - *S.F. MILLER - Caterpillar Tractor Co. 11-24-52*
 Copy No. 155 - *D. C. D. number 6/22/53*
 Copy No. 155 -
 Copy No. 156 - *Nakayama, Kazuyo - Japan - 12-28-53*
 Copy No. 157 -
 Copy No. 158 -
 Copy No. 159 -
 Copy No. 160 -
 Copy No. 161 -
 Copy No. 162 -
 Copy No. 163 -
 Copy No. 164 -
 Copy No. 165 -
 Copy No. 166 -
 Copy No. 167 -
 Copy No. 168 -
 Copy No. 169 -
 Copy No. 170 -
 Copy No. 171 -
 Copy No. 172 -
 Copy No. 173 -
 Copy No. 174 -
 Copy No. 175 - *Mr. S. C. Mackie, Sydney, Nova Scotia. 1 copy 9/25/50*

(Total - 175 copies)

Library of Congress 8/12/54
 NAS-ARC (Library) 8/10/56 - 1 copy

PROGRESS REPORT

Navy Bureau of Ships Contract NObs-31217

Project SR-96

CORRELATION OF LABORATORY TESTS WITH
FULL SCALE SHIP PLATE FRACTURE TESTS:
A STUDY OF STRAIN GRADIENTS.

By: E. P. Klier
F. C. Wagner
J. L. Fisher
M. Gensamer

Mineral Industrial Experiment Station
School of Mineral Industries
The Pennsylvania State College
State College, Pennsylvania

INDEX

	<u>Page</u>
ABSTRACT	i
LIST OF TABLES	ii
LIST OF FIGURES	iii
I - PURPOSE	1
II - INTRODUCTION	1
A - Continuity	
B - Theory	
C - Historical	
D - Facts Bearing on the Problem	
E - Personnel	
III - MATERIALS	4
IV - METHODS OF TEST	4
A - Hardness Tests	
B - Metallographic Tests	
C - X-Ray Analysis	
V - RESULTS AND DISCUSSION	6
A - X-Ray Analysis	
B - Hardness Gradients of Broken Charpy Bars	
C - Hardness Gradients of Bent Charpy Bars	
D - Hardness Gradients of Large Fractured Plates	
E - Metallography	
VI - CONCLUSIONS	14
REFERENCES	15

ABSTRACT

Strain gradients normal to fracture surfaces were determined. These fracture surfaces were developed under the following conditions of test: (1) V-notch Charpy bars broken by impact at various locations within the transition zone, (2) V-notch Charpy bars bent, but not completely broken, by impact above the transition temperature, (3) slow bend Schnadt type bars broken below the transition temperature, and (4) 72-inch wide, center notch, tensile specimens broken with ductile and brittle behavior.

The strain gradients were studied by means of hardness tests, metallographic methods and X-ray analysis.

It is concluded that true cleavage separation is not accompanied by a measurable strain gradient but most "brittle" or "cleavage" fractures, so classified on the basis of gross appearance, contain some areas separated by a shear mechanism.

LIST OF TABLES

		<u>Page</u>
Table 1	- Chemical Composition of the Steels	16
Table 2	- Fracture Phenomena in Charpy V-Notch Test Bars	17
Table 3	- Fracture Phenomena in Large Plate Specimens	18

LIST OF FIGURES

		<u>Page</u>
Figure 1	Idealized Forms of Strain Gradient.	19
Figure 2	X-ray Patterns Steel A.	20
Figure 3	The Fracture Midway Through the Specimen Steel Dr. This is a fully ductile specimen. (cf. Figures 26 & 27).	21
Figure 4	The Fracture Midway Through the Specimen Steel C. This is a fully brittle specimen. (cf. Figures 5 & 6).	22
Figure 5	Hardness Contours - Steel C. Tested at -22°F ; energy absorption 3 ft. lbs.	23
Figure 6	Hardness Gradient - Steel C. Tested at -22°F ; energy absorption 3 ft. lbs.	24
Figure 7	Hardness Contours - Steel E. Tested at 36°F ; energy absorption 7 ft. lbs.	25
Figure 8	Hardness Gradient - Steel E. Tested at 36°F ; energy absorption 7 ft. lbs.	26
Figure 9	The Character of the Fracture at the Base of the Notch Steel E. (cf. Figures 7 & 8).	27
Figure 10	The Fracture Midway Through the Specimen Steel E. (cf. Figures 7 & 8).	28
Figure 11	The Fracture at the Back of the Specimen Steel E. (cf. Figures 7 & 8).	29
Figure 12	Hardness Contours - Steel Dr. Tested at -39°F ; energy absorption 10 ft. lbs.	30
Figure 13	Hardness Gradient - Steel Dr. Tested at -39°F ; energy absorption 10 ft. lbs.	31
Figure 14	Hardness Contours - Steel C. Tested at 50°F ; energy absorption 13 ft. lbs.	32

		<u>Page</u>
Figure 15	Hardness Gradient - Steel C. Tested at 50°F; energy absorption 13 ft. lbs.	33
Figure 16	Hardness Contours - Steel E. Tested at 75°F; energy absorption 16 ft. lbs.	34
Figure 17	Hardness Gradient - Steel E. Tested at 75°F; energy absorption 16 ft. lbs.	35
Figure 18	Hardness Contours - Steel Dr. Tested at 16°F; energy absorption 27.5 ft. lbs.	36
Figure 19	Hardness Gradient - Steel Dr. Tested at 16°F; energy absorption 27.5 ft. lbs.	37
Figure 20	Hardness Contours - Steel Dr. Tested at 64°F; energy absorption 46.5 ft. lbs.	38
Figure 21	Hardness Gradient - Steel Dr. Tested at 64°F; energy absorption 46.5 ft. lbs.	39
Figure 22	Hardness Contours - Steel C. Tested at 113°F; energy absorption 52ft. lbs.	40
Figure 23	Hardness Gradient - Steel C. Tested at 113°F; energy absorption 52 ft. lbs.	41
Figure 24	Hardness Contours - Steel E. Tested at 170°F; energy absorption 54 ft. lbs.	42
Figure 25	Hardness Gradient - Steel E. Tested at 170°F; energy absorption 54 ft. lbs.	43
Figure 26	Hardness Contours - Steel Dr. Tested at 126°F; energy absorption 80.5 ft. lbs.	44
Figure 27	Hardness Gradient - Steel Dr. Tested at 126°F; energy absorption 80.5 ft. lbs.	45

		<u>Page</u>
Figure 28	Hardness Contours - Steel C. Tested at 212 ^o F; energy absorption 80 ft. lbs.	46
Figure 29	Hardness Gradient - Steel C. Tested at 212 ^o F; energy absorption 80 ft. lbs.	47
Figure 30	Hardness Contours - Steel E. Tested at 212 ^o F; energy absorption 70 ft. lbs.	48
Figure 31	Hardness Gradient - Steel E. Tested at 212 ^o F; energy absorption 70 ft. lbs.	49
Figure 32	Hardness Contours - Steel C. Tested at 212 ^o F; angle of bend = 9 ^o , no crack formed. Kinetic Energy of Hammer = 13 ft. lbs.	50
Figure 33	Hardness Contours - Steel C. Tested at 212 ^o F, angle of bend = 22 ^o , small crack formed. Kinetic Energy of Hammer = 34 ft. lbs.	51
Figure 34	Hardness Contours - Steel C. Tested at 212 ^o F, angle of bend = 38 ^o , crack through 1/3 of section. Kinetic Energy of Hammer = 54 ft. lbs.	52
Figure 35	Photograph of Plate C-3.	53
Figure 36	Line Drawing of Plate C-3.	54
Figure 37	Hardness Contours - Specimen No. 1, Plate C-3.	54
Figure 38	Hardness Contours - Specimen No. 2, Plate C-3.	55
Figure 39	Hardness Contours - Specimen No. 3, Plate C-3.	55
Figure 40	Hardness Contours - Specimen No. 4, Plate C-3.	56
Figure 41	Photograph of Plate 22-1K.	57
Figure 42	Line Drawing of Plate 22-1K.	58
Figure 43	Hardness Contours - Specimen No. 1, Plate 22-1K.	58

		<u>Page</u>
Figure 44	Hardness Contours - Specimen No. 2, Plate 22-1K.	59
Figure 45	Hardness Contours - Specimen No. 3, Plate 22-1K.	59
Figure 46	Hardness Contours - Specimen No. 4, Plate 22-1K.	60
Figure 47	Hardness Contours - Specimen No. 5, Plate 22-1K.	60
Figure 48	Photograph of Plate N-1-A.	61
Figure 49	Line Drawing of Plate N-1-A.	62
Figure 50	Hardness Contours - Specimen No. 1, Plate N-1-A.	62
Figure 51	Hardness Contours - Specimen No. 2, Plate N-1-A.	63
Figure 52	Hardness Contours - Specimen No. 3, Plate N-1-A.	63
Figure 53	Hardness Contours - Specimen No. 4, Plate N-1-A.	64
Figure 54	Deformation Twins in Steel C. Nital Etch x 600.	65
Figure 55	Strain Lines in Steel Dr. Nital Etch x 600	66
Figure 56	The Fracture for Specimen No. 4 Plate 22-1K showing Deformation Twins and Transition from Brittle to Ductile Failure. Nital Etch x 500.	67
Figure 57	The Fracture for Specimen No. 5 Plate 22-1K showing Brittle cracks of inter-and intra-granular types. Nital Etch x 500.	68
Figure 58	Another Region for Specimens No. 5 Plate 22-1K. Nital Etch x 500.	69
Figure 59	Character of the Fracture in Specimen No. 4 Plate 22-1K. Nital Etch x 500.	70

I PURPOSE

The purpose of this investigation was to determine the characteristics of the strain gradient at brittle fractures and at ductile fractures.

II INTRODUCTION

A-Continuity

In the Progress Report¹ of September 15, 1946 it was indicated that a report was being prepared relating to the study of strain gradients as revealed by hardness measurements on impact bars fractured at various levels of energy absorption. This initial work has been expanded to include (1) comparable tests on large fractured plates (2) X-Ray analyses of strain at fractured surfaces and (3) metallographic examination of fractured sections. All of the above work is reported here.

B - Theory

In attempting to rationalize the difference between brittle and ductile behavior in steel, it has been suggested that important information might be gained by an extensive study of strain gradients normal to the fracture surface. This suggestion is based on two facts: (1) a ductile fracture is associated with a much higher energy absorption than a brittle fracture and (2) the intensity and extent of plastic strain are indices of the energy absorption. Thus a study based on fact (2) could conceivably provide data to explain fact (1), which is the essence of the brittle ship plate problem.

Since it is known that the energy absorbed by plastic straining increases with both the volume of strained metal and the intensity of the strain, it

(1) - Numbers refer to items in Bibliography

follows that brittle behavior, as contrasted with ductile behavior, must be associated with either (1) a smaller volume of strained metal or (2) lower strain intensity. Figure 1 schematically illustrates these two possible differences between ductile and brittle fractures.

In Figure 1(a), the strain intensity at the fracture surface is represented as being constant for all fractures, brittle and ductile. But the ductile fracture is represented by the gradual strain gradient, and will, therefore, be associated with a large volume of strained metal and consequently a large energy absorption; the brittle fracture is represented by the steep strain gradient and will, therefore, be associated with a small volume of strained metal and consequently a small energy absorption. Thus Figure 1(a) illustrates alternative (1) above. Alternative (2) is illustrated by Figure 1(b). Here, the strain intensity at the fracture surface is represented as being high for ductile fractures and low for brittle fractures. Since energy absorption increases with intensity of plastic strain, it follows that the fracture associated with high strain intensity will absorb a large amount of energy and will be ductile, while the fracture associated with the low strain intensity will not absorb much energy, and will be brittle.

(Figure 1 and the subsequent data of this report assume strain to be a linear function of hardness. While this is not strictly true, it is a satisfactory approximation, and strain gradients are represented in this report by hardness gradients).

C - Historical

The extent of plastic strain in the impact test has been studied by Sauerwald and Wieland², Moser³ and others^{4, 5, 6}. Reviews of the notch impact

test have been made by Fettweiss⁷ and MacGregor and Fisher⁸. A study of these works reveals the following:

- (1) No extensive analysis of straining has been undertaken by methods of high sensitivity. Thus details about the volume of strained metal may have escaped detection.
- (2) No correlated analysis of the volume of strained metal developed at various points in the transition region has been published. This is an important gap to be filled.

The present work is intended to supply data on both of these points.

D - Facts Bearing on the Problem

Due to the character of matter, any substance, to a greater or less extent, will function as a diffraction grating for X-rays. In all instances of diffraction, the same fundamental factors are operative, but optimum conditions obtain when the material to be investigated has a well developed space lattice. When such is the case, and disregarding the effects of grain size, well defined maxima in the diffraction spectra arise for a given type of space lattice at rigorously defined diffraction angles. Many factors contribute to the final appearance of the individual spectral lines, but those factors which alter the appearance of a given line as a function of plastic strain are somewhat limited. This would serve to decrease the uncertainty in the evaluation of a given pattern except that, unfortunately, no one-to-one correspondence has ever been ascertained as existing between any of the factors measured and the degree of plastic strain. For instance, the obtaining of diffused lines which is frequently taken as indicating a state of plastic strain can result from chemical composition gradients, elastic strain gradients, particle size and, certainly not least

important, external geometry of the diffracting surface. In the examination of a fracture surface this last factor may be a most important factor, which usually cannot be modified. The effects of elastic strain gradients are most certainly present in a plastically deformed metal, while particle size may well be important.

E - Personnel

The staff participating in this work consisted of:

M. Gensamer,	Technical Representative
E. P. Klier	Investigator
J. L. Fisher	Investigator
F.C. Wagner	Investigator
J. O. Mack	Investigator
M. A. Bishop	Research Assistant
Selma Krause	Drafting
Mina Moessen	Technical Labor
P. Vonada	Technical Labor
H. Colyer	Technical Labor

III MATERIALS

Detailed information on the steels used will be found in earlier reports^{1,9}. Chemical analyses are contained in Table I.

Three sections of 72-inch wide plates which had been broken by the center notch tensile test in the course of previous investigations⁹ are shown by Figures 35, 41 and 48. Specimens from these plates were used for hardness contour surveys.

IV METHOD OF TEST

A-Hardness

Standard LH (longitudinal specimens with the notch perpendicular to the plate surface) V-notch Charpy bars were broken at temperatures selected to cover the entire transition zone. Temperatures, energies and fracture

appearances are listed in Table II.

After fracturing, the bars were nickel plated to preserve the fracture surface and were sectioned on the center plane perpendicular to the notch. The half specimens were next mounted in a plastic which set at room temperature, and were polished. Finally, a regular pattern of indentations was made on the polished surface using a Vickers diamond and a 1000 g. load on a Tukon hardness testing machine. Preliminary tests had shown that these conditions of test would eliminate any effects of grain orientation, but would preclude an approach to the fracture closer than 0.01 inches. This degree of sensitivity is adequate to reveal macroscopic detail of the strain gradient. Preparation and testing of specimens from the large fractured plates was done in like manner.

These hardness data were plotted on a scaled likeness of the specimens and lines connecting points of equal hardness were drawn. This process gave a hardness contour map and, consequently, an approximate strain contour map. In order to permit representation of the hardness gradient in a more easily visualized manner, the linear hardness gradients at the base of the notch and at a point midway through the fracture, were determined and plotted.

Three Charpy specimens of steel C were tested in the conventional manner except that the hammer was not raised to its full height, but rather to a height insufficient to cause complete fracture of the bars. The hammer rebounded after striking the bar, but was arrested before it could strike the bar a second time. Conditions of test were as follows:

	<u>Test A</u>	<u>Test B</u>	<u>Test C</u>
Temperature °F	212	212	212
K. E. of Hammer	13	34	54
Bend Angle	9°	22°	38°
Crack	None	Very Shallow	1/3 through Bar

These specimens were sectioned, mounted, polished and tested as described above.

B-Metallography

Microsections were made of all specimens, and photomicrographs of the impact specimens were taken at the notch, midway through the bar and at the back side. Microstructural evidence of Neumann Bands, strain lines and grain deformation was observed and recorded.

C-X-Ray Analysis

Specimens of steel C representing the virgin metal, a brittle fracture surface and ductile fracture surfaces were used. In order to insure a clean and complete break at the fracture surfaces, the Schnadt type bar was used and was broken by the slow bend technique. A Sachs type camera with both cassette and specimen stationary was used. Exposures were made with K α radiation.

V - RESULTS AND DISCUSSION

A - X-Ray Tests

The X-ray data are presented in Figure 2. Pattern (a) is for the virgin metal. The point of interest is the resolved doublet leading to two lines on the pattern (α_1 and α_2). These lines are typical and are used as reference lines. Patterns (b), (c), (d), and (e) were taken on ductile fracture surfaces. From the lack of resolution of the doublet it may be stated that extensive strain exists at the fracture surface. Finally in pattern (f), taken on a brittle

fracture surface, the doublet is resolved as in pattern (a). This means that the strain, if it exists for the brittle fracture, was insufficient to be picked up by this X-ray diffraction technique. Since it is estimated that the X-ray procedure used will reveal a strain gradient of .0001 inch thickness, it is indicated that a strain gradient, if it exists adjacent to the brittle fracture surface, must be no thicker than 0.0001 inch. A gradient of this extent could, under no circumstances, lead to high energy absorption in its development. From this it follows that for practical purposes, the strain gradient construction presented in Figure 1b conforms with the experimental results.

Additional information in terms of metallographic data pertain to this point. Thus, in Figure 3, the fracture surface is typical of a ductile failure. The metallographic structure shows a highly torn and deformed zone at the fracture edge. This zone appears to be of the order of .01 inch thick. This region rapidly passes into a zone of much lower plastic strain, a zone, however, in which plastic strain is still appreciable, as indicated by the distorted grains. In Figure 4 the fracture presented is a brittle fracture. There is no evidence of plastic strain accompanying this fracture. The metallographic data, therefore, are in full agreement with the X-ray data for the consideration of the "ideal" brittle and ductile types of failure. Additional data concerning the metallography of what might be considered intermediate types of failure are presented in subsequent sections.

The X-ray and metallographic data which have been presented argue against acceptance of the strain gradient type presented in Figure 1a. By elimination the strain gradient type presented in Figure 1b appears to describe the conditions at the fracture surface.

B-Hardness Gradients of Broken Charpy Bars

Hardness gradient data are presented in Figures 5 to 8 and 12 to 34, in the forms of contour maps and linear gradients at the notch and at the center of the Charpy specimens. These data will be considered in groups based on similarity of energy absorption and position in the transition zone.

Group 1 - Low Energy Absorption, (<7 ft. lbs.) Figures 5,6,7, and 8. The specimen of steel C (Figures 5 and 6) with an energy absorption of 3 ft. lbs. would be considered "100% granular" by conventional usage. The hardness contour indicates very slight strains at the notch and under the tup, but the crack itself was not accompanied by strain which was discernible by the hardness measuring technique used. These same remarks apply to the specimen of steel E (Figures 7 and 8), with the exceptions that this fracture showed slightly more shear under the tup and greater strain at this location. Photomicrographs of this specimen (Figures 9, 10, and 11) are in agreement with the hardness data. It is evident that the crack in this specimen was completed before the major part of the straining occurred. This follows from the fact that it would not be possible to strain an uncracked specimen at the tup without causing a corresponding strain at the notch. Hence, most of the strain at the tup must have resulted from bending of the specimen after completion of the brittle portion of the crack.

Group 2 - Medium Low Energy Absorption (10-16 ft. lbs.) Figures 12-17. The hardness contours of this group are similar to those of group 1 with the exception the strain at the notch and the tup is greater, and consequently the length of the brittle crack through unstrained metal is shorter. The same analysis of straining prior to, and after, formation of the brittle crack applies. Notice that the brittle portion of the crack is still not accompanied by a macroscopic strain gradient.

Group 3 - Medium High Energy Absorption (27.5 - 54.0 ft. lbs.) Figures 18-25. The hardness contours of this group are similar to those of groups 1 and 2 with the exceptions that the zones of strain at the notch and the tup are still greater and are extended sufficiently, at 45° to the specimen axis, to contact each other beneath the crack. (e.g. Figure 18). There still exist regions of brittle fracture, however, showing no macroscopic strain gradient, with the possible exceptions of curves B in Figures 16 and 23. These slight strain gradients likely result from the appreciable bending which occurred prior to the formation of the crack rather than from a mechanism accompanying the brittle crack. Note the marked rise of the B curves, which obviously reflects the extension of the strained zones at the notch and tup.

Group 4 - High Energy Absorption (>70 ft. lbs.) Figures 26-31. These fractures were fully ductile ones. The hardness contours show that the region of no strain at the center of the bars has vanished. However, the intensity of the strain at the center of the bars is still much lower than it is near the notch and tup.

These strain gradient studies of broken Charpy bars lead to three observations:

a - A ductile crack in a Charpy bar is not accompanied by a distinctive and uniform macroscopic strain gradient, for if it were, the A and B curves of the totally ductile fractures would be alike.

b - A brittle crack in a Charpy bar can be propagated through either strain-free, or slightly strained material, without imposition of a macroscopic strain gradient.

c - The macroscopic strain gradients of a broken Charpy bar largely reflects the strain resulting from bending actions rather than any crack propagation phenomena.

C-Hardness Contours of Bent Charpy Bars

The hardness contours of the three Charpy bars which were struck by a Charpy hammer possessing energy insufficient to cause complete fracture are shown in Figures 32, 33, and 34.

Figure 32 illustrates the distribution of the strain prior to crack formation for conditions of test under which ductile fracture would occur if energy sufficient to effect fracture were available. Notice the steep strain gradient under the notch and, to a lesser degree, at the top, and the strain free metal near to the neutral axis.

Figure 33 differs from Figure 32 in degree only with the exception that a shallow ductile crack extends from the notch.

In Figure 34, the bending action has proceeded sufficiently to cause strain at the center of the bar, and the ductile crack is extended further into the material strained by bending. The strain distribution and intensity resemble those of Figure 28, which represents the same steel tested at the same temperature but with energy which was sufficient to cause total fracture.

D - Hardness Gradients in Large Fractured Plates.

It is evident, from results presented above, that the strain gradients in broken Charpy bars are largely reflections of the amount of bending prior and subsequent to the formation of the crack. Consequently, it was realized early in the course of this investigation that fractures which had occurred under the action of tensile forces only should be included in the strain gradient studies. For this reason, specimens from 72-inch wide plates, which had been fractured in the center notch tensile test, were examined.

Plate C-3 will be considered first. From the chevron marks (Figure 35)

it is evident that this plate failed with a "brittle" crack terminating at the notch. Figure 36 indicates orientations and locations of the hardness survey specimens. Figures 37-40 show the hardness contours, from which two significant observations can be made:

(1) Some portions of this "brittle" crack are not accompanied by a discernible macroscopic strain gradient, i.e., the base hardness of the plate extends unchanged to the crack surface.

(2) Some portions of this "brittle" crack are accompanied by fairly steep and shallow strain gradients, which can occur in the center of the plate (e.g. Figure 39) but which are especially marked at the plate surface (e.g. Figure 40).

These observed facts compel the conclusion that those locations on the crack which are unaccompanied by a strain gradient were cracks indeed prior to the separation of the material at those locations on the crack which are accompanied by a strain gradient. The most obvious of the possible explanations for this marked variation in the strain gradients at different locations on the same "brittle" crack is that the reduced constraint resulting from the growth of the crack allowed appreciable plastic strain at the locations which were last to separate. But in any event, these specimens indicate that a crack, which would be classified as "brittle" by conventional criteria, may or may not be accompanied by a macroscopic strain gradient.

Plate 22-1K is shown in line drawing by Figure 42. From its photograph, Figure 41, it is evident that the crack was "ductile" from the notch to the location of specimen No. 4, thence "brittle" to the plate edge. With the additional observation that the ductile portions of this crack show the expected strain gradient, (Figures 43-47) the remarks pertaining to plate previously discussed apply.

Plate N-1-A is shown in line drawing by Figure 48. From its photograph, Figure 48, it is evident that the crack originated at the notch and extended in the "ductile" mode for approximately 1/2 inch before changing to the "brittle" mode. It should be noted⁹ that this plate was unusual in that it absorbed approximately 1/3 of the maximum energy observed for a totally "ductile" specimen of the same material. The strain gradients of those specimens near the notch, Figures 50, 51, and 52, closely resemble findings from the previous two plates. Figure 53, however, which represents "brittle" behavior, differs markedly from the other "brittle" contours in its demonstration of definite and uniformly developed macroscopic strain gradient. In this respect, Figure 53 is not unlike previously discussed contour maps which represent "ductile" behavior (cf. Figure 43), with the exception that the gradient slope does not sharply increase in steepness near to the fracture. It is suggested that the "brittle gradient" of Figure 53 might be related to the unusually high energy absorption, in that it could be reflecting general straining in a zone between the notch and the plate edge rather than a strain incidental to, or necessary for, propagation of the crack.

E - Metallography

Results of metallographic examination are presented in Tables 2 and 3, and in Figures 3, 9 to 11, and 54 to 59.

In the tables, fracture types are listed as "brittle," "ductile," and "brittle-ductile." The last mentioned designation indicates uncertainty as to the type of behavior. It should be emphasized that these classifications are based on metallographic data only.

Figures 9, 10, and 11, respectively, illustrate the microstructures of sections which intersect the crack at the base of the notch, midway through the

bar and at the back of the bar, of a "brittle" specimen (steel E, 36⁰E). The strain gradients of this specimen are represented by Figures 7 and 8. It can be seen that the hardness data and microstructures are in agreement, with the exception that microstructure (Figure 9) shows evidence of considerable plastic strain in a very restricted zone at the base of the notch, which strain is not evident in the hardness contour (Figure 7). This "disagreement" unquestionably reflects the greater sensitivity of metallographic examination, as compared with the hardness tests, and strongly suggests that the strain gradients at ductile fractures are actually much steeper and reach much higher strain values very near (< 0.01 ") to the crack surface than is indicated by the hardness contours. Figure 10 clearly demonstrates the total lack of any metallographic manifestations of strain at a clean cleavage separation.

Figures 54 and 55, respectively illustrate deformation twins and strain lines, not necessarily typical, occurring in broken Charpy bars.

Figure 56 represents the location in plate 22-1-K at which the crack changed from the "ductile" to the "brittle" mode. Note the typical evidence of an appreciable strain gradient adjacent to the ductile part and the clean, strain-free cleavage adjacent to the brittle part of the crack.

Figure 57 represents a "brittle" location of the crack in plate 22-1-K. The previously mentioned characteristics of a cleavage fracture are illustrated. Note also the typical trans-crystalline path, which is interrupted by a very short inter-crystalline separation at the pearlite grain near crack midpoint.

Figure 58 illustrates the above mentioned characteristics of a cleavage crack and in addition, reveals interesting behavior of the crack in the ferrite grain near its midpoint. Notice how the crack branch was arrested within the ferrite grain.

Figure 59 represents a cleavage crack. Of interest is the deformation of the ferrite fragments which evidently suffered considerable strain, although the crack caused no discernible strain in the main body of the ferrite or pearlite grains.

VI CONCLUSIONS

- 1 - The strain gradient at some locations on any "brittle" crack, if it exists indeed, is so restricted as to depth that it is not detectable by X-ray or metallographic tests.
- 2 - The strain gradients at some locations on most "brittle" cracks is not characteristically different from the strain gradients of a "ductile" crack.
- 3 - Fractures which would be classified as "brittle" by conventional usage, e.g., by gross appearance, generally display both of the above two types of strain gradients.
- 4 - Figure 1(b) schematically represents the difference between separation by shear and separation by cleavage with respect to strain gradients, except that the cross-hatched area should be immeasurably small.

REFERENCES

1. Progress Report - Research Project SR-96, Serial No. SSC-9, Contract NObs-31217 dated March 19, 1947.
2. F. Sauerwald and H. Wieland: Z. Metallk. 17 (1925) p. 358/63 and 392/9; St. und Eisen 46 (1926) p. 546.
3. M. Moser: Krupp'sche Monatsh. 2 (1921) p. 225/40. St. und Eisen 42 (1922) p. 90/7; Z. V. D. I. 67 (1922) p. 43.
4. R. Hinzmann: Dissertation. Techn. Hochsch. Berlin, 1925.
5. F. Schüle: Material prüf. Anst. a.d. Eidg. Techn. Hochschule Zürich 1913, Vol. 10a. p. 1/16; St. und Eisen 34 (1914) p. 1266.
6. F. Schüle and E. Brunner: Intern. Verb. Kopenhagener Kongress 1909 III. 2.p 1/6; St. und Eisen 29 (1909) p. 1453.
7. F. Fettweiss: Archiv für Eisenhüttenwesen April 1929, Vol. 10, p. 660.
8. C. W. MacGregor and J. C. Fisher: Jrnl. Applied Mechanics 11 March (1944) p. A28/A34.
9. Final Report - Research Project SR-92, Serial No. SSC-8, Contract NObs-31222, dated January 1947.
10. Final Report - Research Project SR-93, Serial No. SSC-10, Contract NObs-31224, dated June 1947.
11. C. S. Barrett: Structure of Metals p. 305. McGraw-Hill Book Company, New York (1943).

TABLE I

Chemical Compositions of the Steels

<u>STEEL</u>	<u>THERMAL TREATMENT</u>	<u>%C</u>	<u>%Mn</u>	<u>%Ni</u>
A	As-rolled	0.26	0.50	0.02
C	As-rolled	0.24	0.48	0.02
Dr	As-rolled	0.22	0.55	0.16
E	As-rolled	0.20	0.33	0.15
C-3-A	Same as C above			
22-1K	Same as Dr above			
N-1-A	As-rolled	0.17	0.53	3.39

TABLE II

Fracture Phenomena in Charpy V-Notch Test Bars

Spec.	Steel	Test Temp. °F	E.A. #	Fracture Type and Location			Deformation Structure and Location		
				Notch	Center	Back	Notch	Center	Back
KRI-5	Dr	-40	10	B ¹	B	B-D	N.B. ³	N.B.	S.L.
KRA-1	Dr	-9	27.5	D ²	B	D	S.L. ⁴	N.B.	S.L.
KRG-4	Dr	18	46.5	D	B	D	S.L.	N.B.	S.L.
KRF-6	Dr	52	80.5	D	D	D	S.L.	S.L.	S.L.
I-28	C	-30	3	B	B	B	N.E.	N.B.	N.B.
I-5	C	25	34	D	B	D	S.L.	N.B.(?)	S.L.
I-2	C	45	52	D	B	D	S.L.	N.B.	S.L.
I-19	C	98	80	D	B-D	D	S.L.	S.L.	S.L.
RRH-3	E	2	7	B	B	B-D	N.B.	N.B.	N.B. & S.L.
RRB-1	E	24	16	B-D	B	B	S.L.	N.B.	N.B.
RRC-3	E	77	54	D	B-D	B-D	S.L.	N.B.	S.L.
RRI-1	E	100	70	D	D	D	S.L.	S.L.	S.L.

1 - B = Brittle

2 - D = Ductile

3 - N.B. = Neumann Bands (deformation twins)

4 - S.L. = Strain Lines

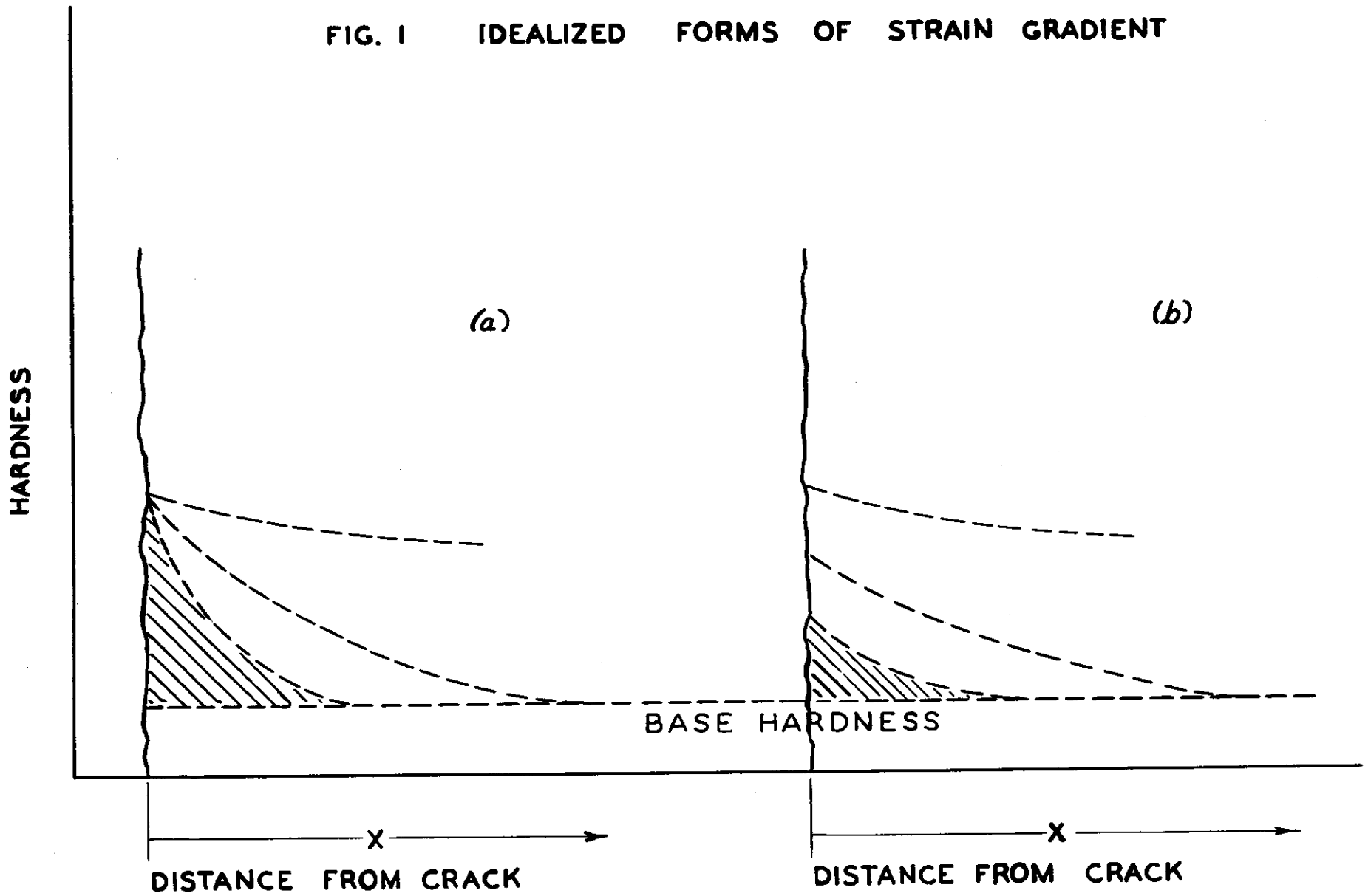
TABLE III

Fracture Phenomena in Large Plate Specimens

Spec.	Temp. °F	Fracture Type & Location ⁶			Deformation Structure & Location		
		1.	2.	3.	1.	2.	3.
NIA(1) ⁶	-55	D ¹	D	D	—	—	—
NIA(2)	to	D	D	D	S.L. ³	S.L.	S.L.
NIA(3)	-51	D	D	D	—	—	—
NIA(4)		B ²	B	B	—	—	—
C-3(1)	101	B	B	B-D	—	—	S.L.
C-3(2)	to	B	B	B	—	N.B. ⁵ & S.L.(r)	N.B.
C-3(3)	104	B	B	B-D	—	N.B.	N.B. & S.L.(r)
C-3(4)		B	B	B	S.L.	N.B.	S.L.
22-1K(1)		D	D	D	S.L.	S.L.	S.L.
22-1K(2)		D	D	D	S.L.	S.L.	S.L.
22-1K(3)		D	B-D	B-D	S.L.	—	—
22-1K(4)		B-D	B	B	S.L.(r) ⁴	Tears	—
22-1K(5)		B	B	B	—	—	N.B.

- 1 - D = Ductile
- 2 - B = Brittle
- 3 - S.L. = Strain Lines
- 4 - S.L.(r) = Strain Lines highly restricted
- 5 - N.B. = Neumann bands (deformation twins)
- 6 - Specimen number and location may be taken from appropriate line drawing (figures 36, 42, and 49). Locations 1, 2, and 3 are left, center and right portions of transverse specimens looking in direction of crack propagation; they denote left, center and right portions of longitudinal specimens with the notch to the left.

FIG. 1 IDEALIZED FORMS OF STRAIN GRADIENT



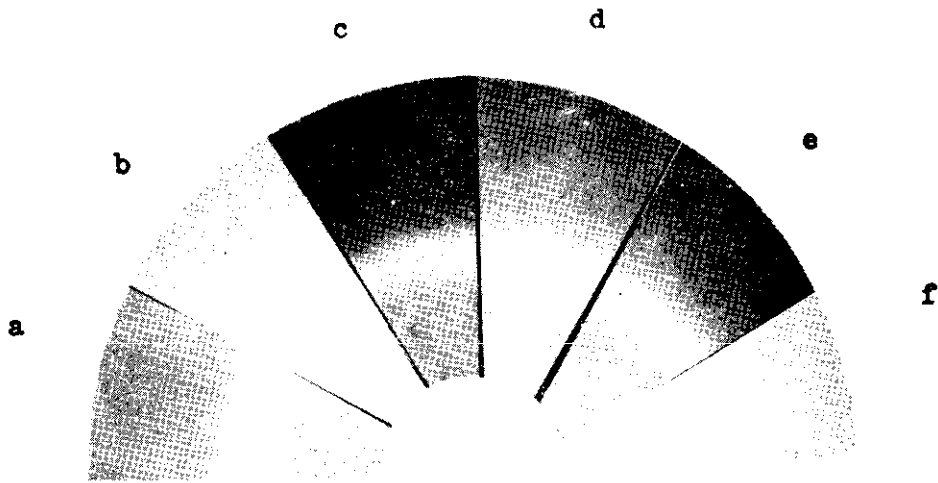


Fig. 2 - X-ray Patterns Steel A

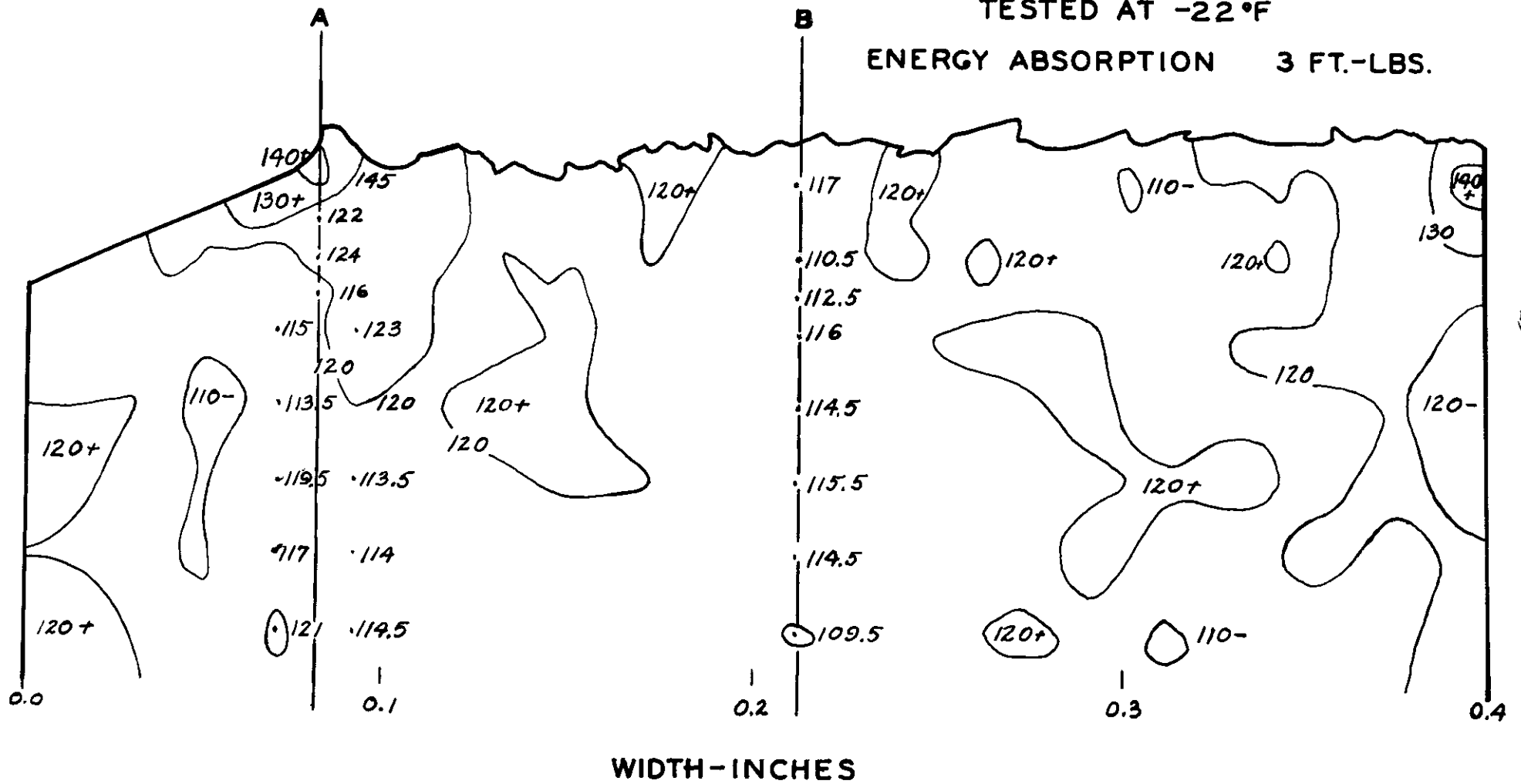


Fig. 3 - The Fracture Midway Through the Specimen Steel Dr.
This is a fully ductile specimen. (Cf. Fig. 26 & 27)
Nital Etch x 600.



Fig. 4 - The Fracture Midway Through the Specimen Steel C.
This is a fully brittle specimen. (Cf. Fig. 5 & 6)
Nital Etch x 600.

FIG. 5
 DPH CONTOURS STEEL C
 V-NOTCH SPECIMEN
 TESTED AT -22°F
 ENERGY ABSORPTION 3 FT.-LBS.



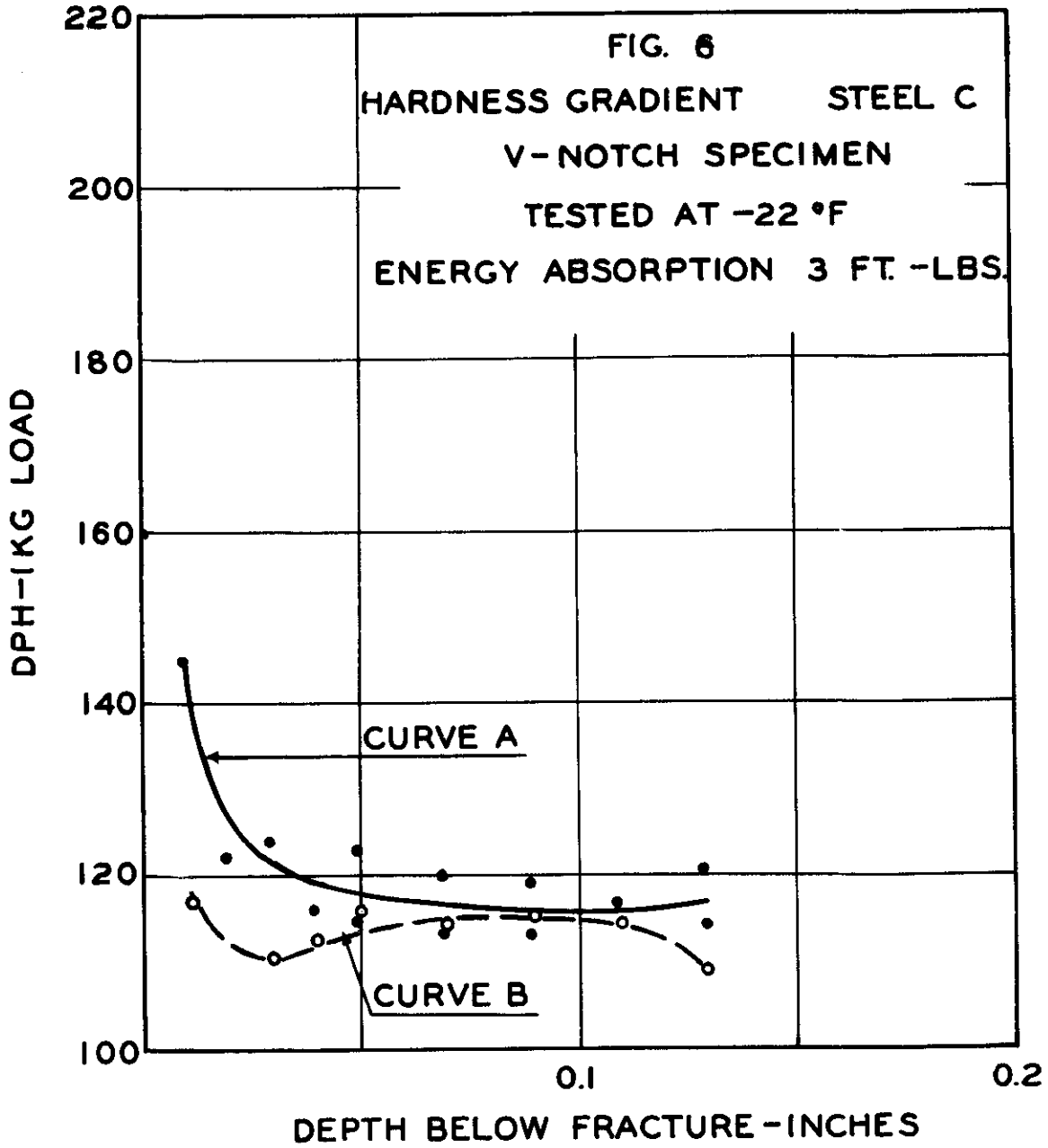


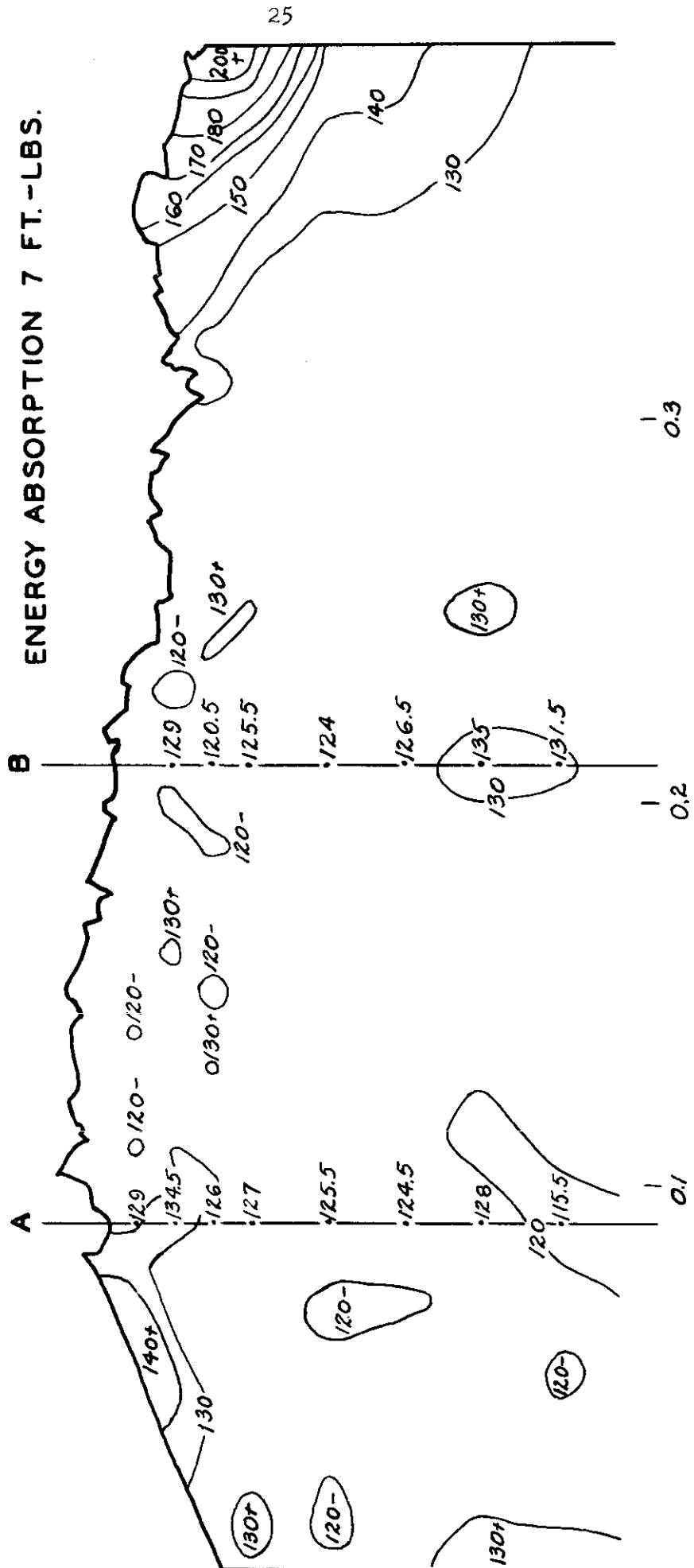
FIG. 7

DPH CONTOURS STEEL E

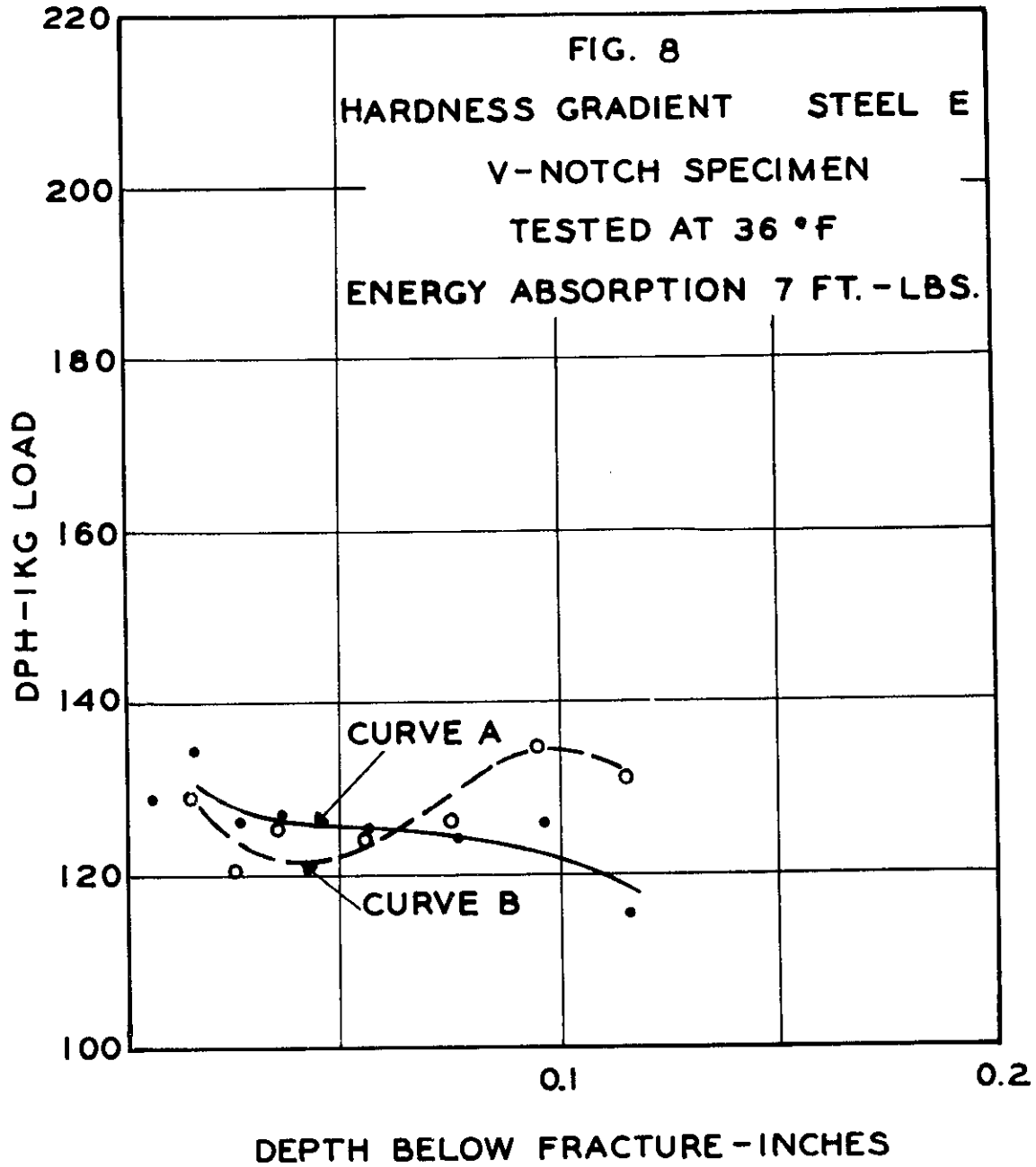
V-NOTCH SPECIMEN

TESTED AT 36 °F

ENERGY ABSORPTION 7 FT.-LBS.



WIDTH - INCHES



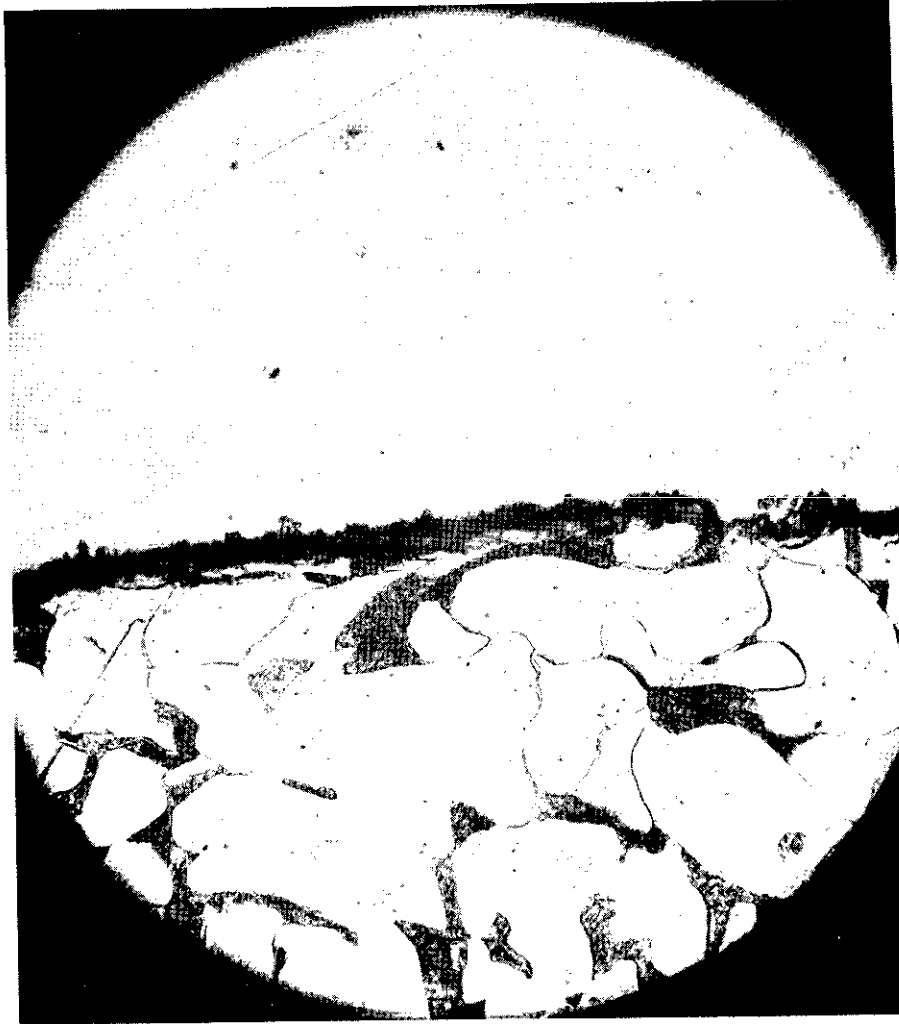


Fig. 9 - The Character of the Fracture at the Base of the Notch Steel E. (Cf. Fig. 7 & 8). Nital Etch x 600.

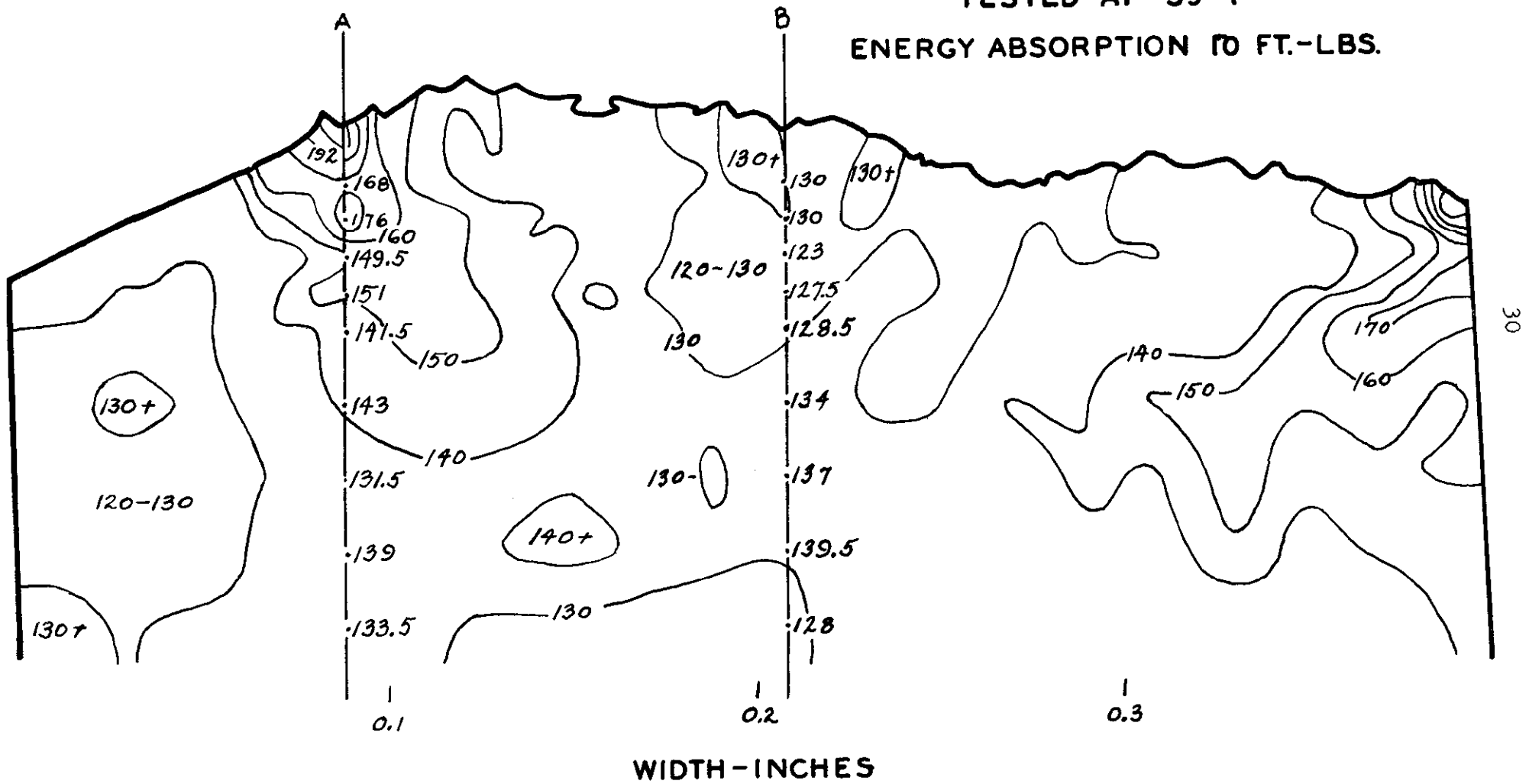


Fig, 10 - The Fracture Midway Through the Specimen Steel E.
(Cf. Fig. 7 & 8). Nital Etch x 600.



Fig. 11 - The Fracture at the back of the Specimen Steel E.
(Cf. Fig. 7 & 8). Nital Etch x 600.

FIG. 12
 DPH CONTOURS STEEL Dr
 V-NOTCH SPECIMEN
 TESTED AT -39°F
 ENERGY ABSORPTION TO FT.-LBS.



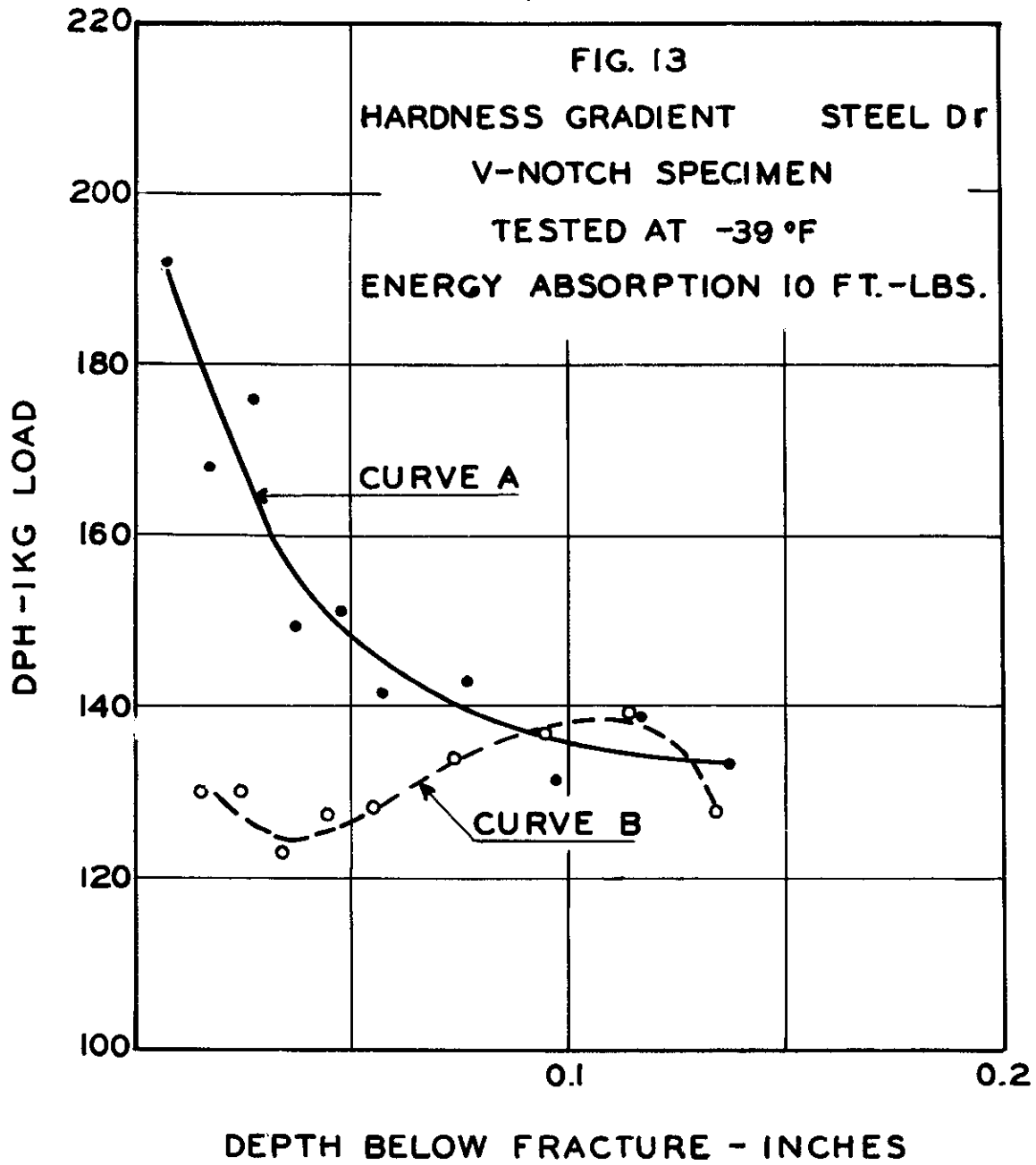
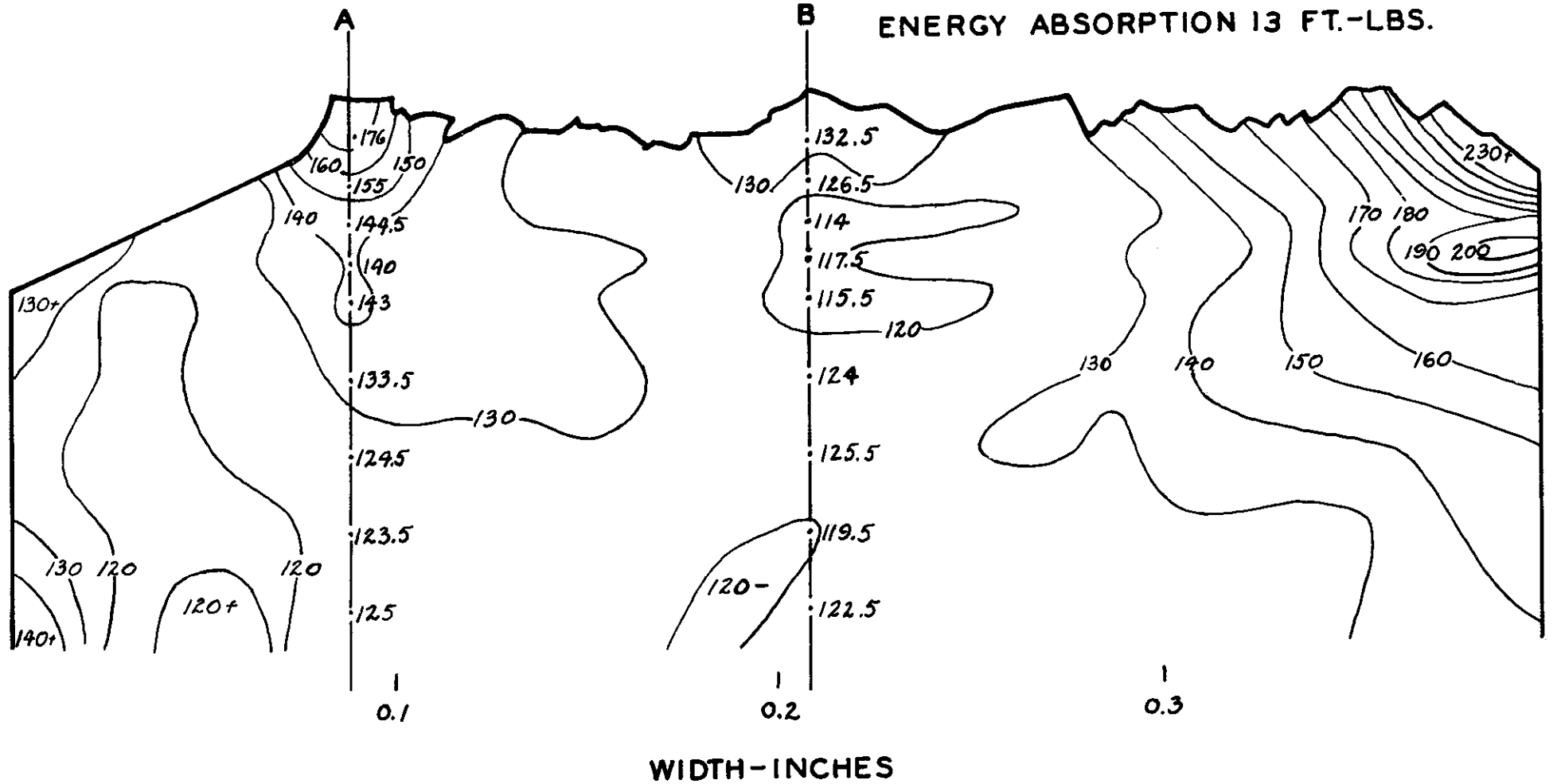


FIG. 14
 DPH CONTOURS STEEL C
 V-NOTCH SPECIMEN
 TESTED AT 50 °F
 ENERGY ABSORPTION 13 FT.-LBS.



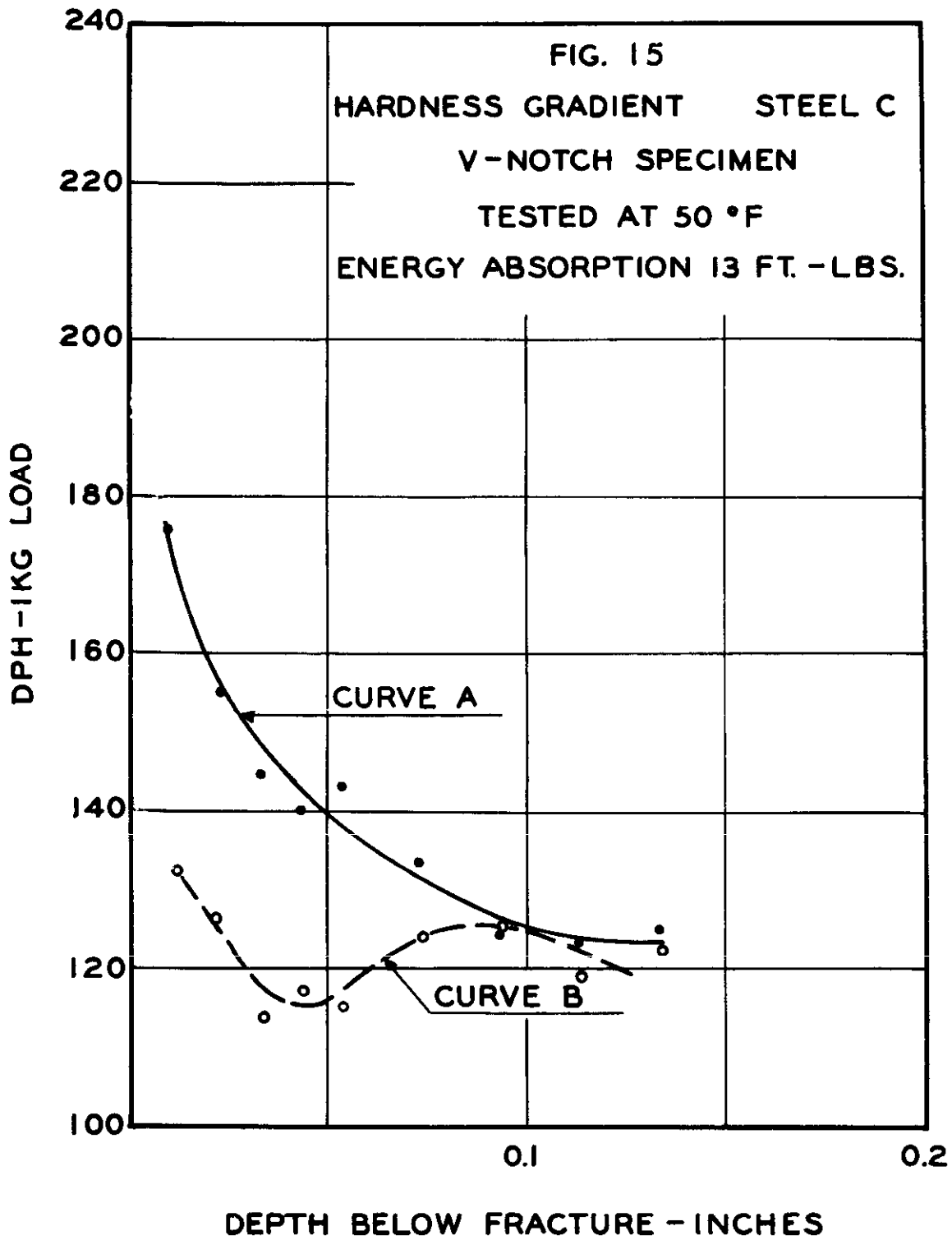
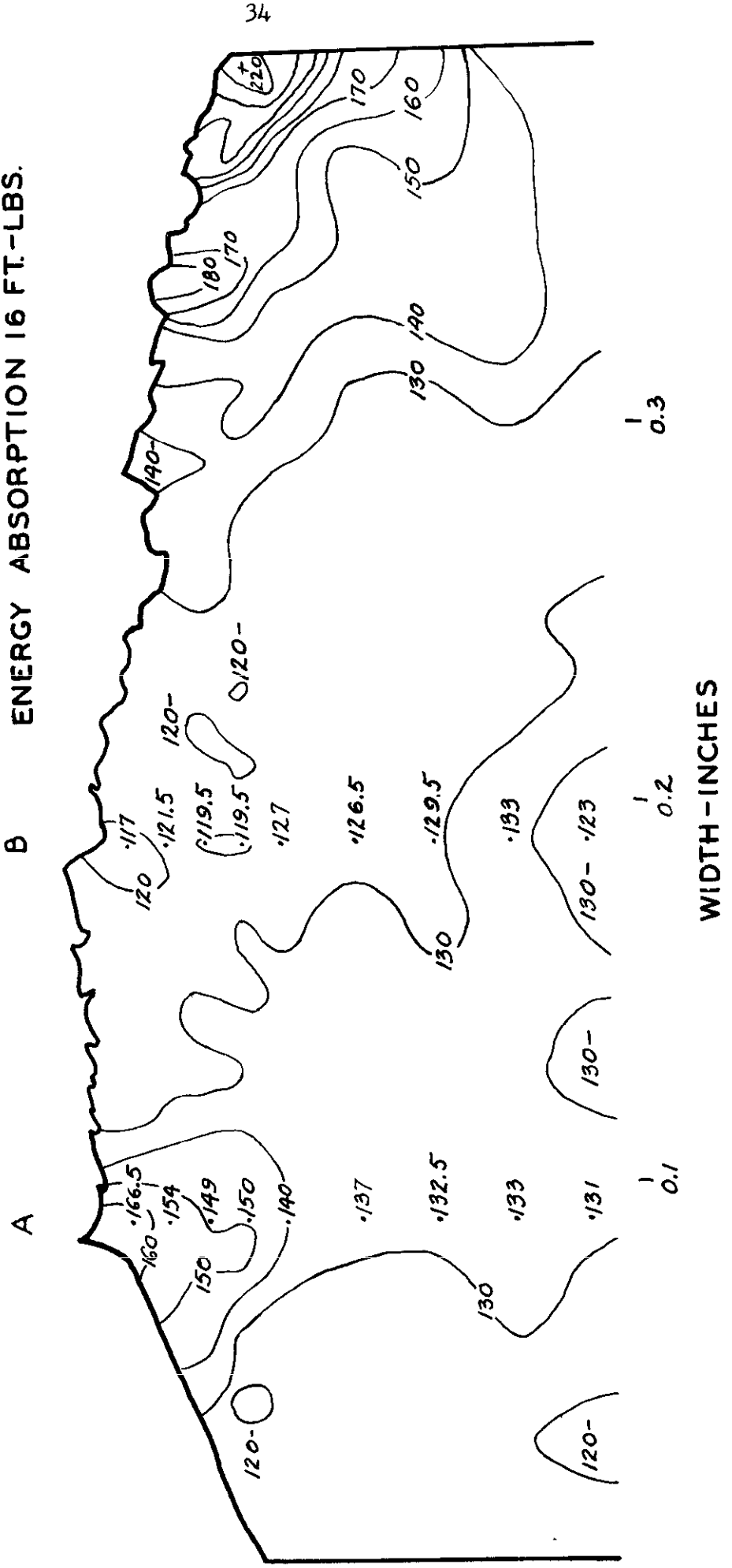


FIG. 16
 DPH CONTOURS STEEL E
 V-NOTCH SPECIMEN
 TESTED AT 75 °F
 ENERGY ABSORPTION 16 FT.-LBS.



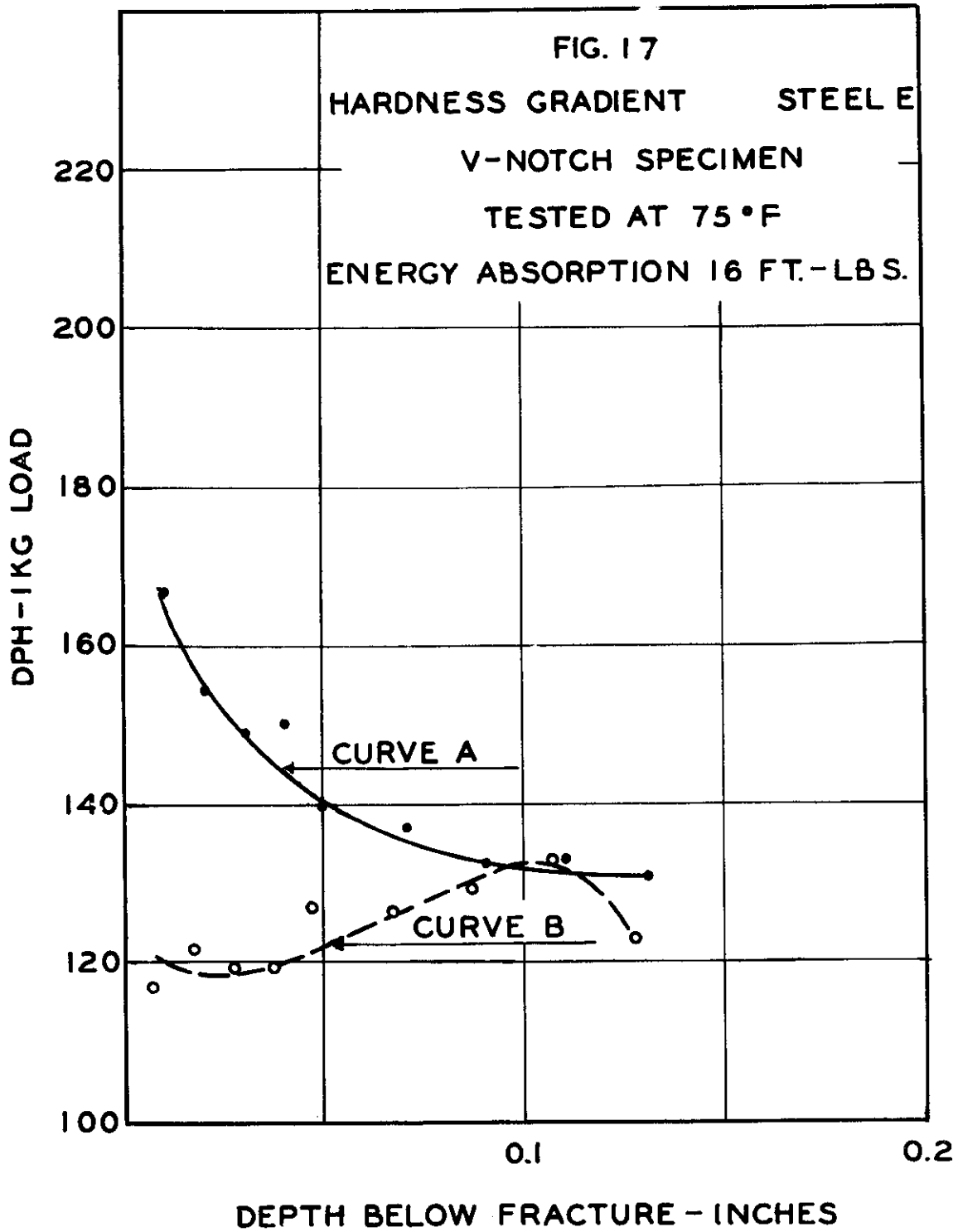
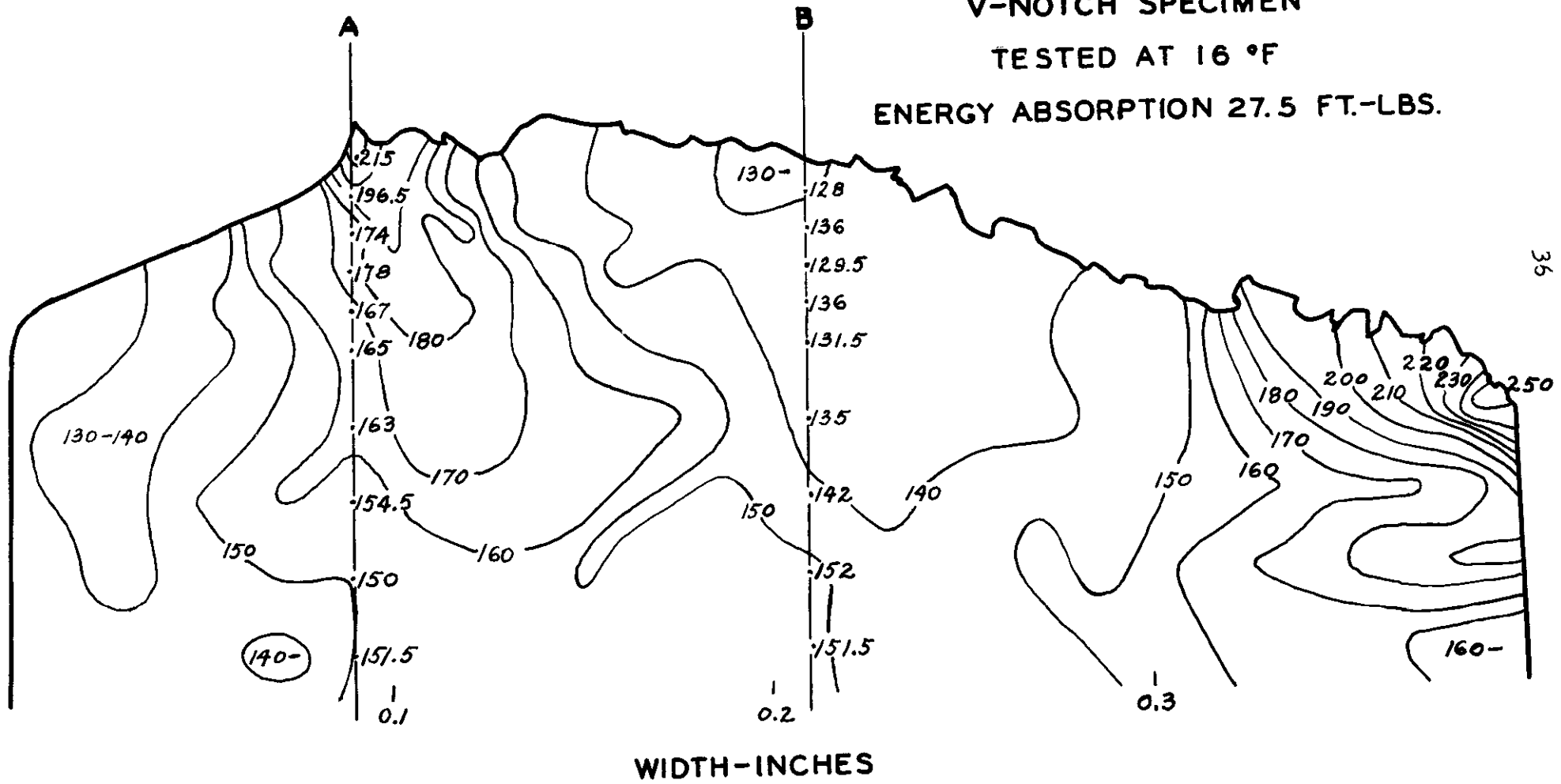


FIG. 18
 DPH CONTOURS STEEL DR
 V-NOTCH SPECIMEN
 TESTED AT 16 °F
 ENERGY ABSORPTION 27.5 FT.-LBS.



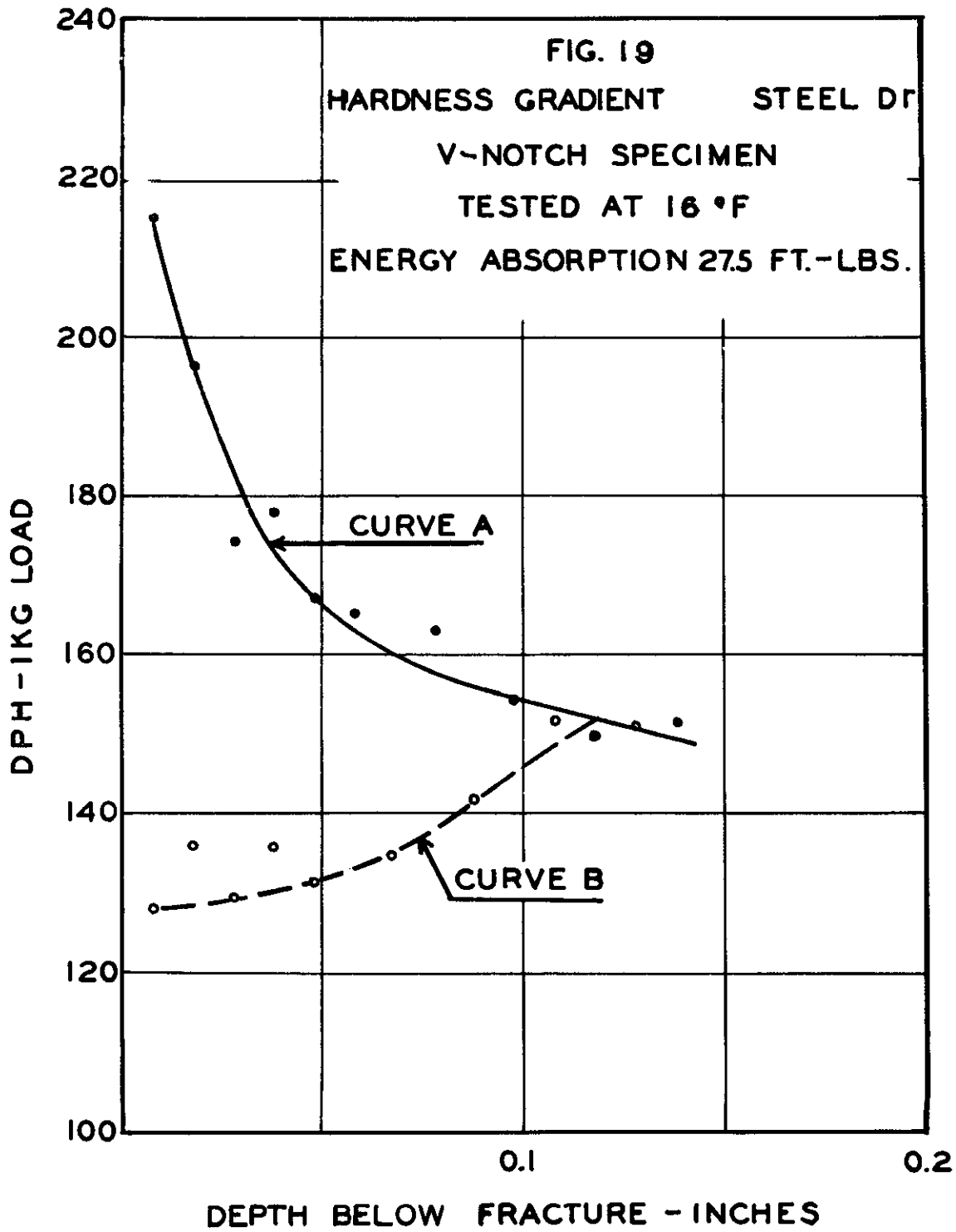
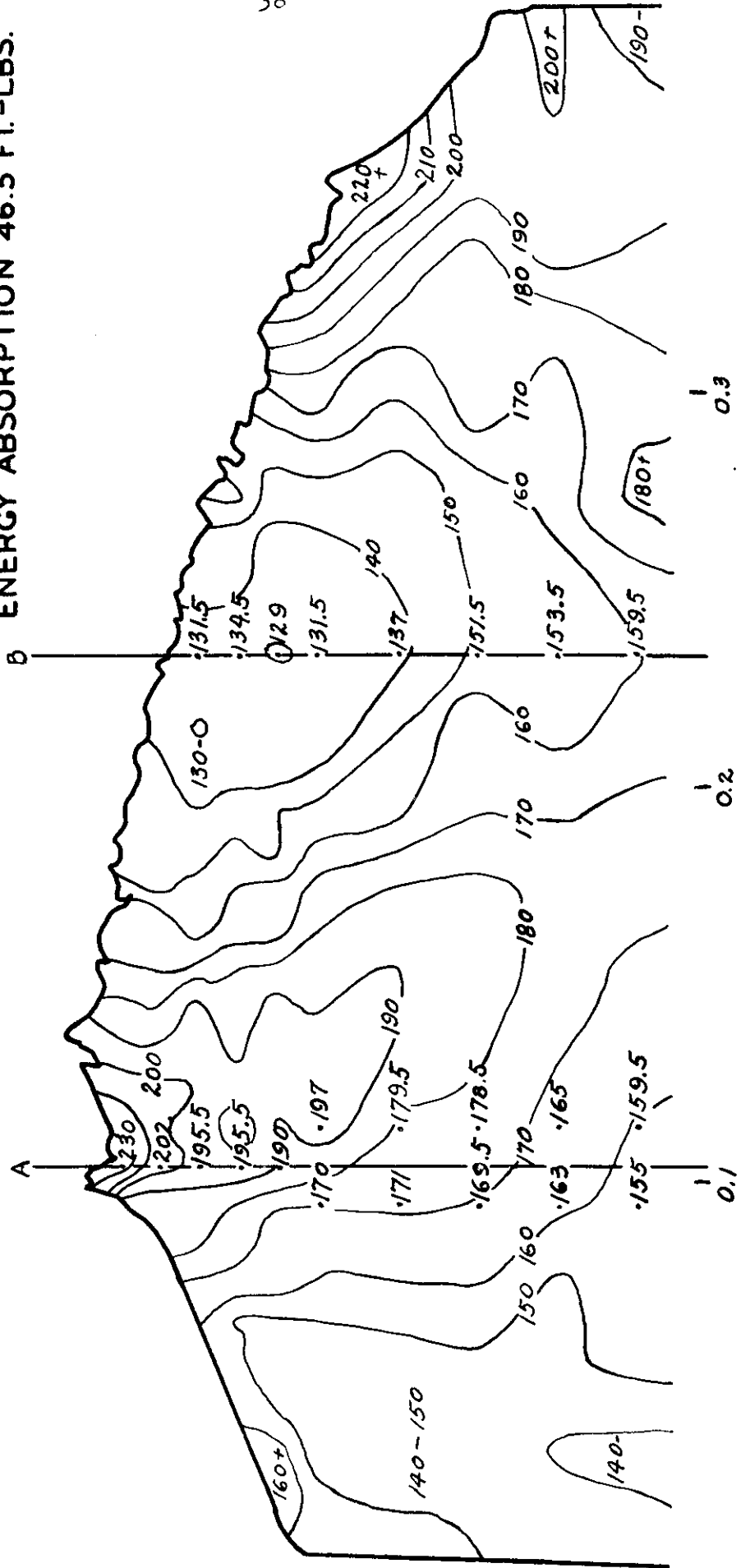


FIG. 20

DPH CONTOURS
STEEL DF
V-NOTCH SPECIMEN

TESTED AT 64°F
ENERGY ABSORPTION 46.5 FT.-LBS.



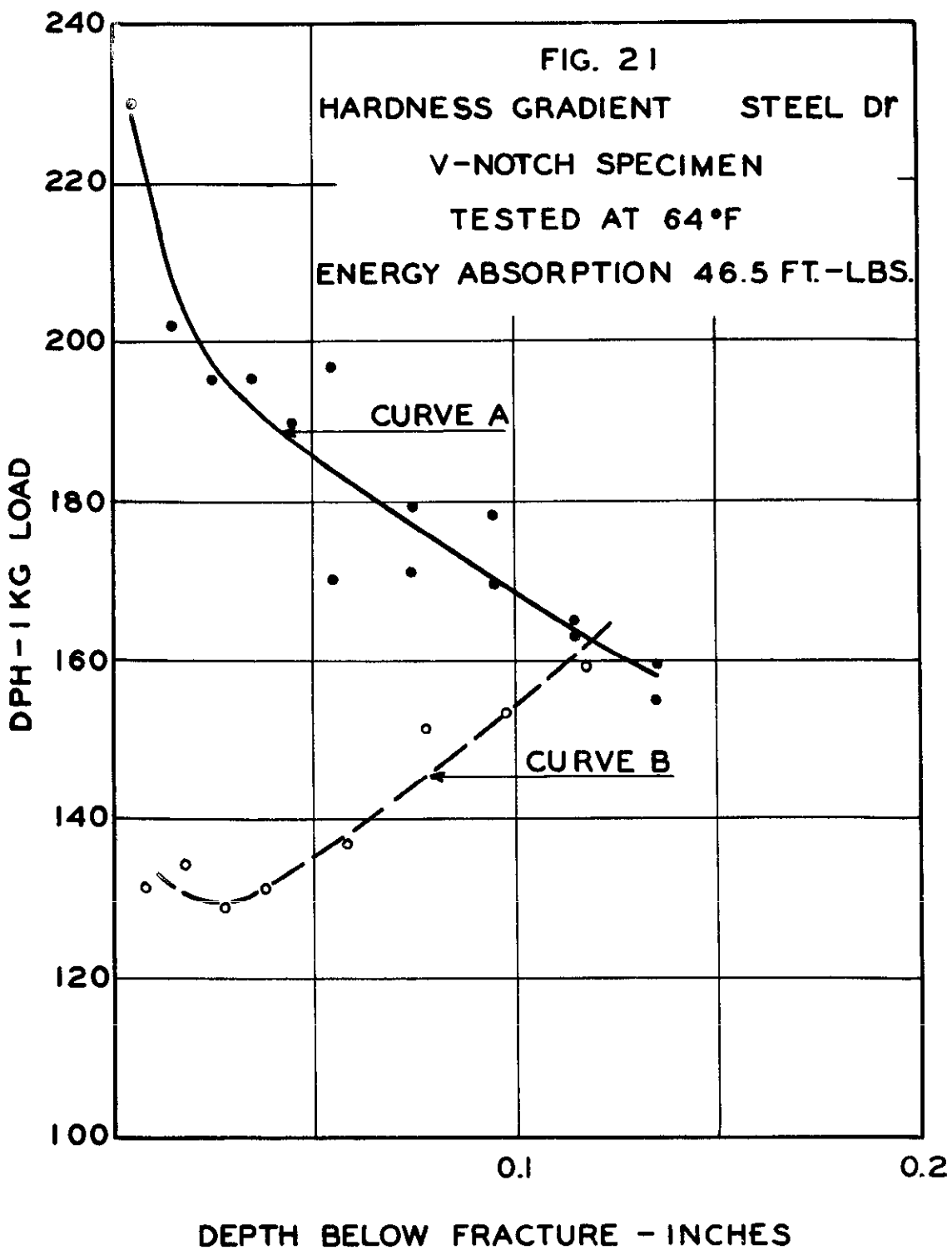
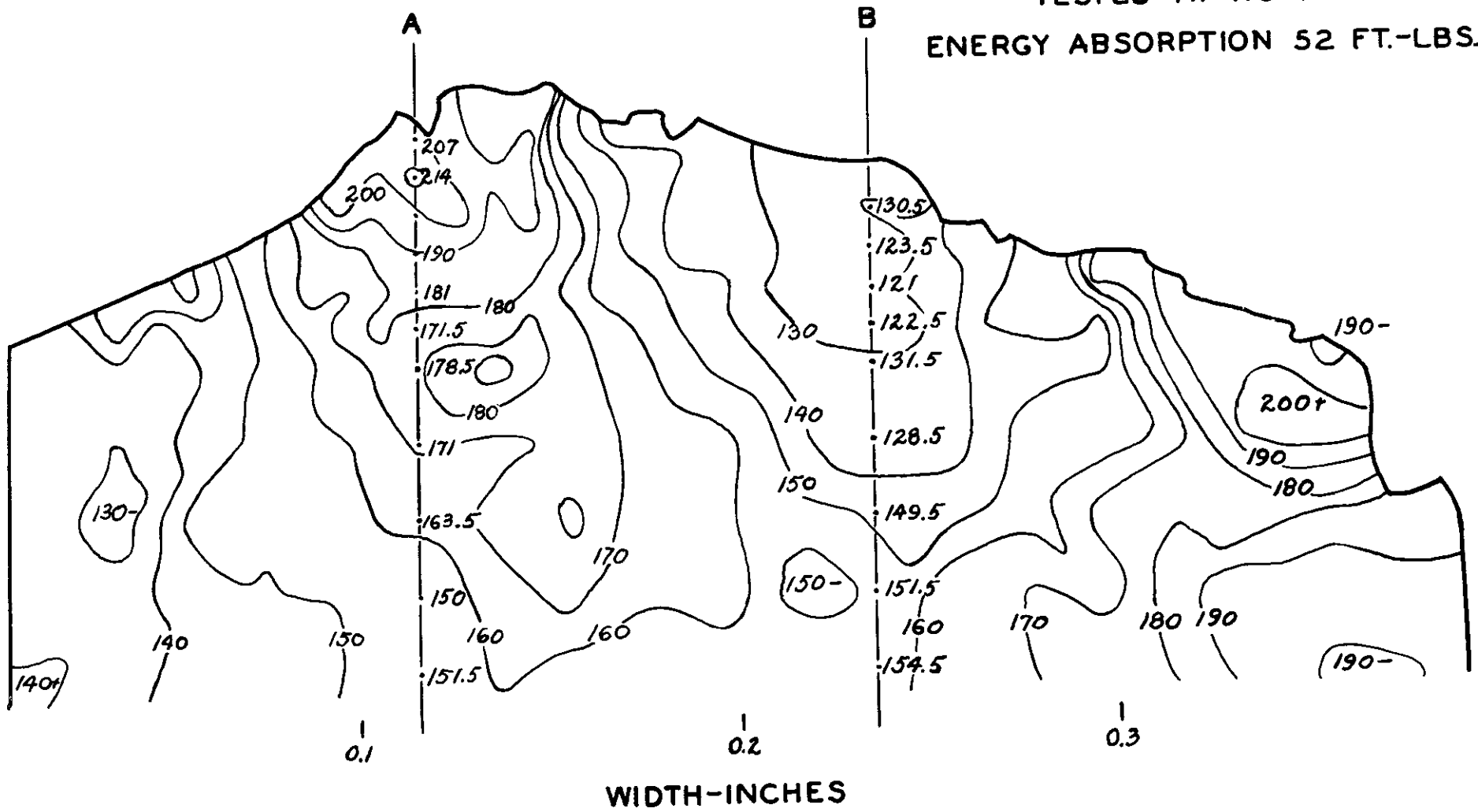


FIG. 22
 DPH CONTOURS STEEL C
 V-NOTCH SPECIMEN
 TESTED AT 113 °F
 ENERGY ABSORPTION 52 FT.-LBS.



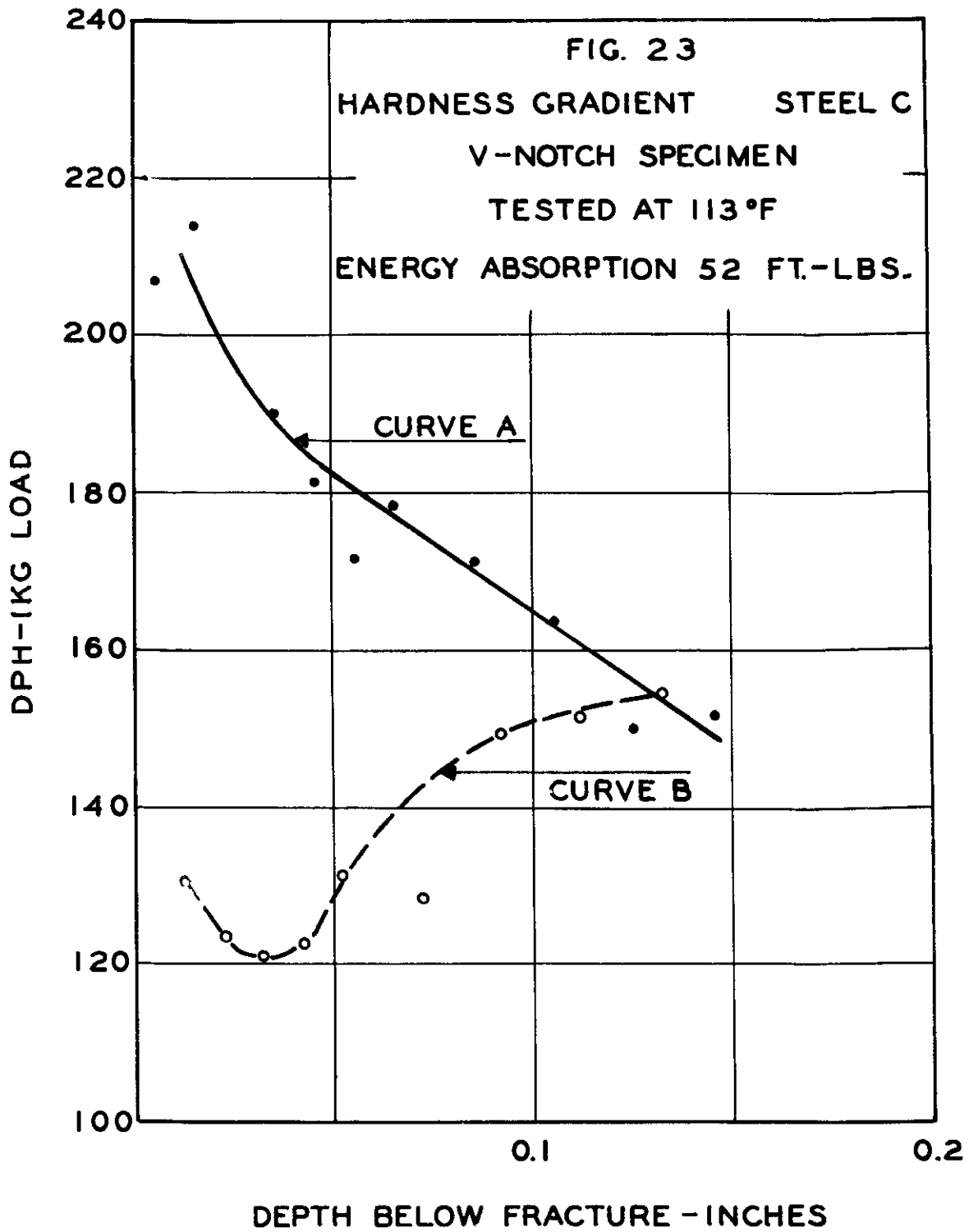
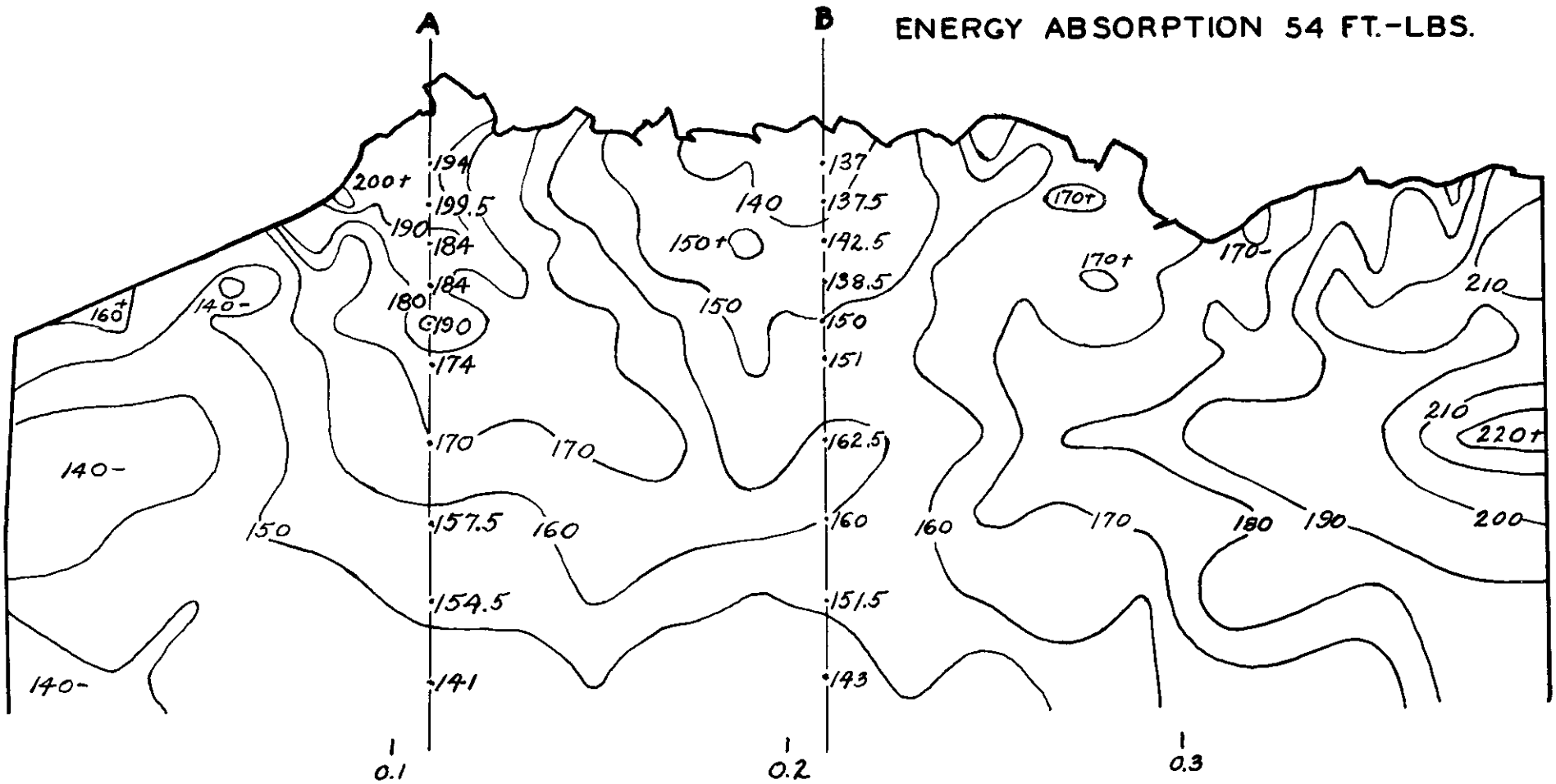


FIG. 24
 DPH CONTOURS STEEL E
 V-NOTCH SPECIMEN
 TESTED AT 170 °F
 ENERGY ABSORPTION 54 FT.-LBS.



WIDTH-INCHES

12

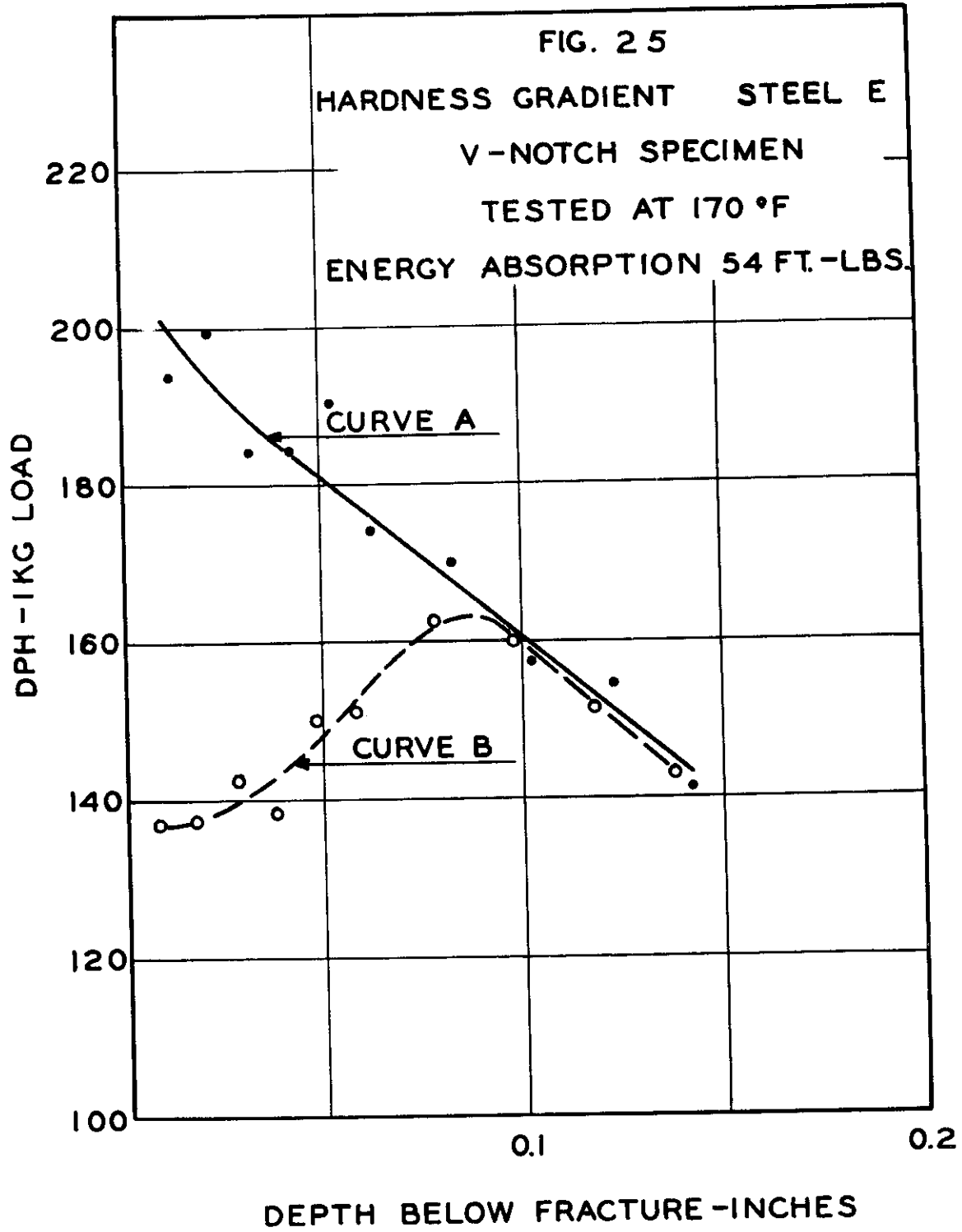
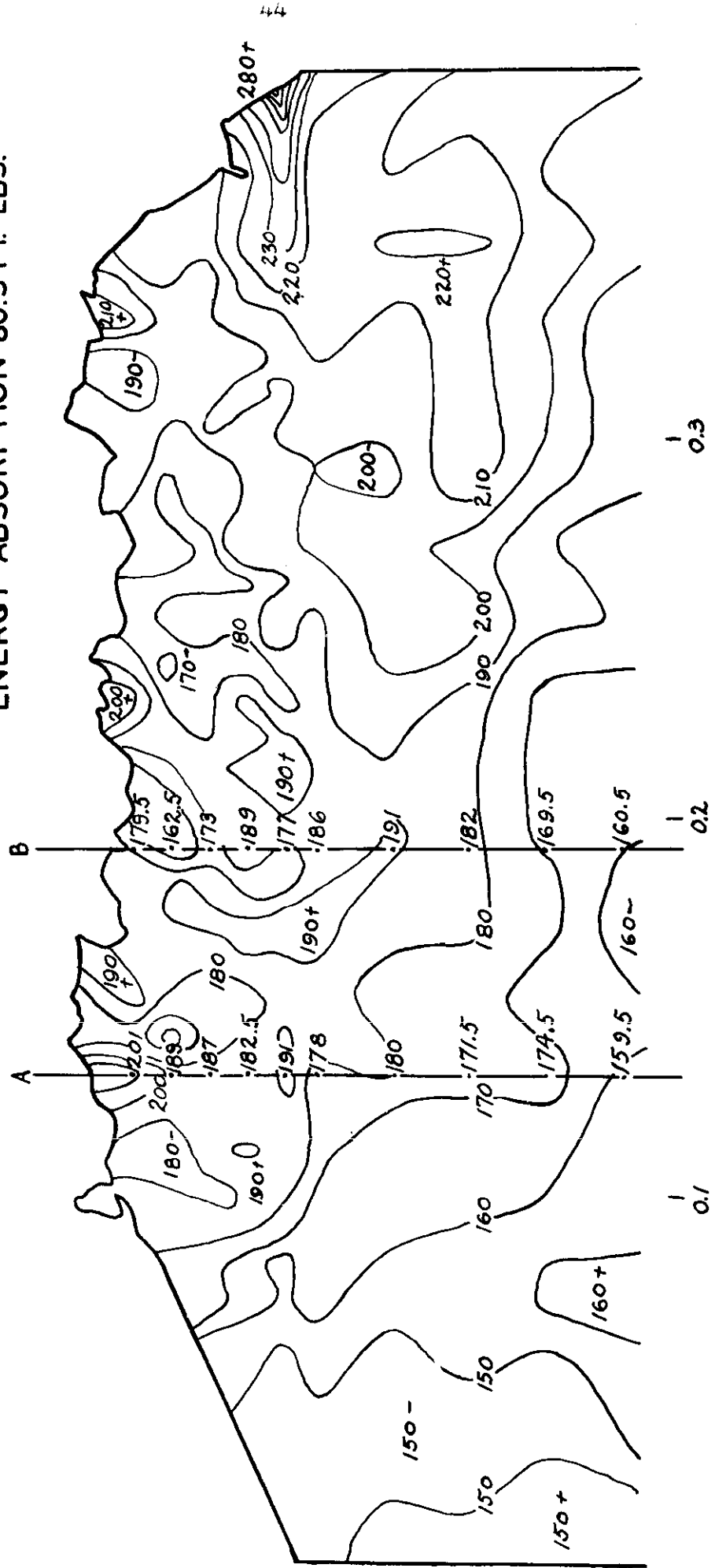


FIG. 2 6
 DPH CONTOURS STEEL DR
 V-NOTCH SPECIMEN
 TESTED AT 126 °F

ENERGY ABSORPTION 80.5 FT.-LBS.



WIDTH - INCHES

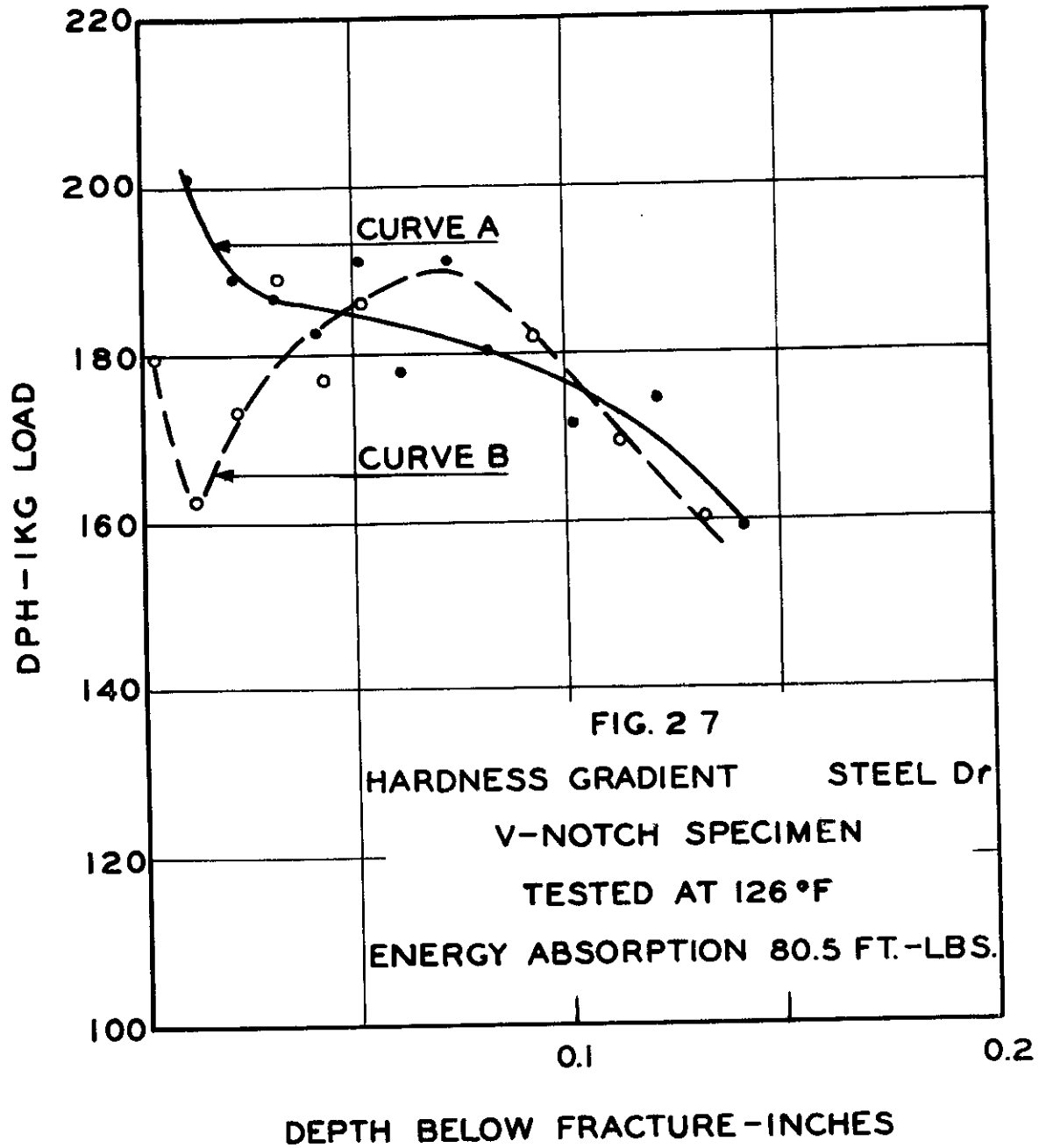
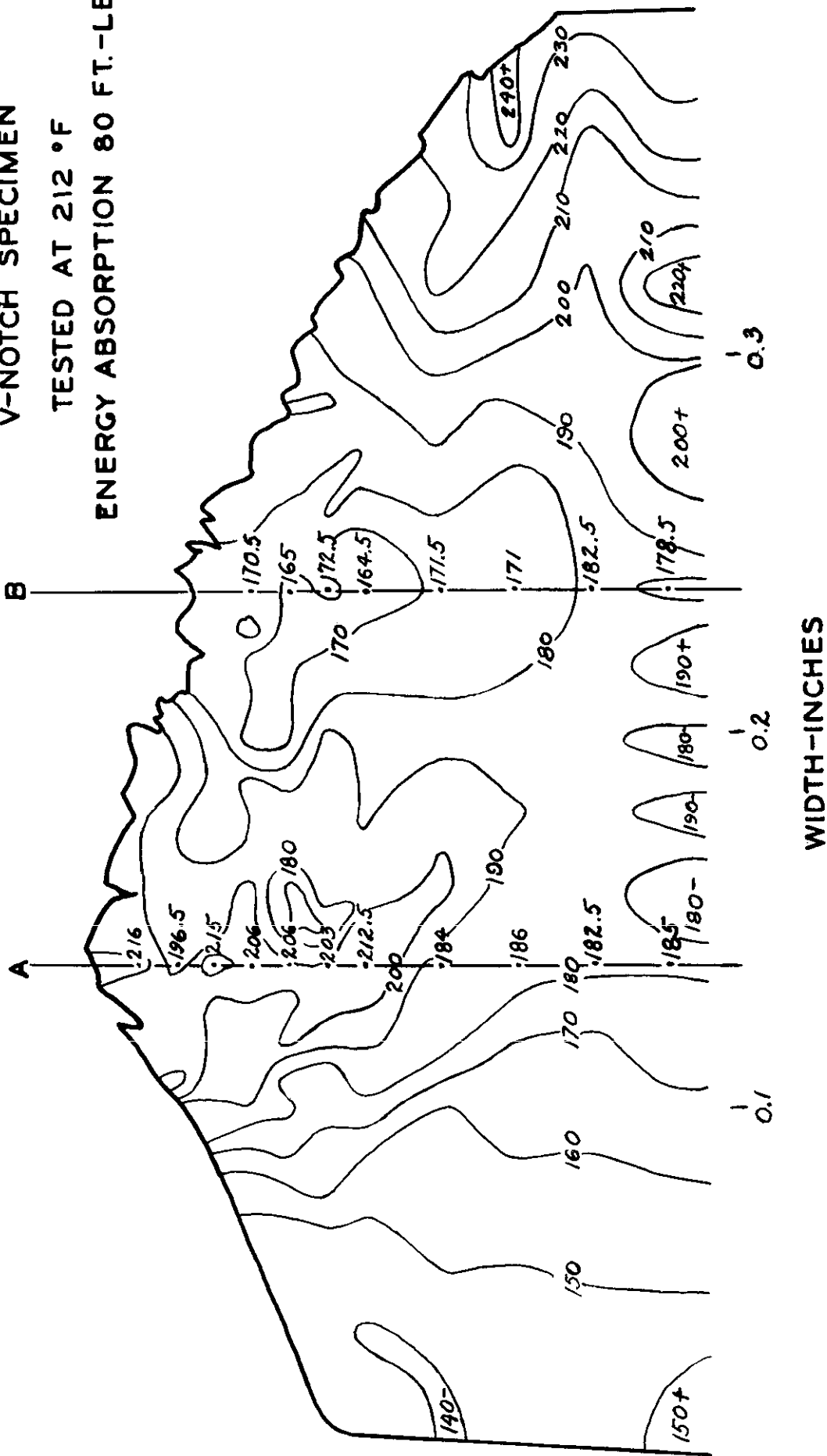


FIG. 28
DPH CONTOURS STEEL C
V-NOTCH SPECIMEN
TESTED AT 212 °F
ENERGY ABSORPTION 80 FT.-LBS.



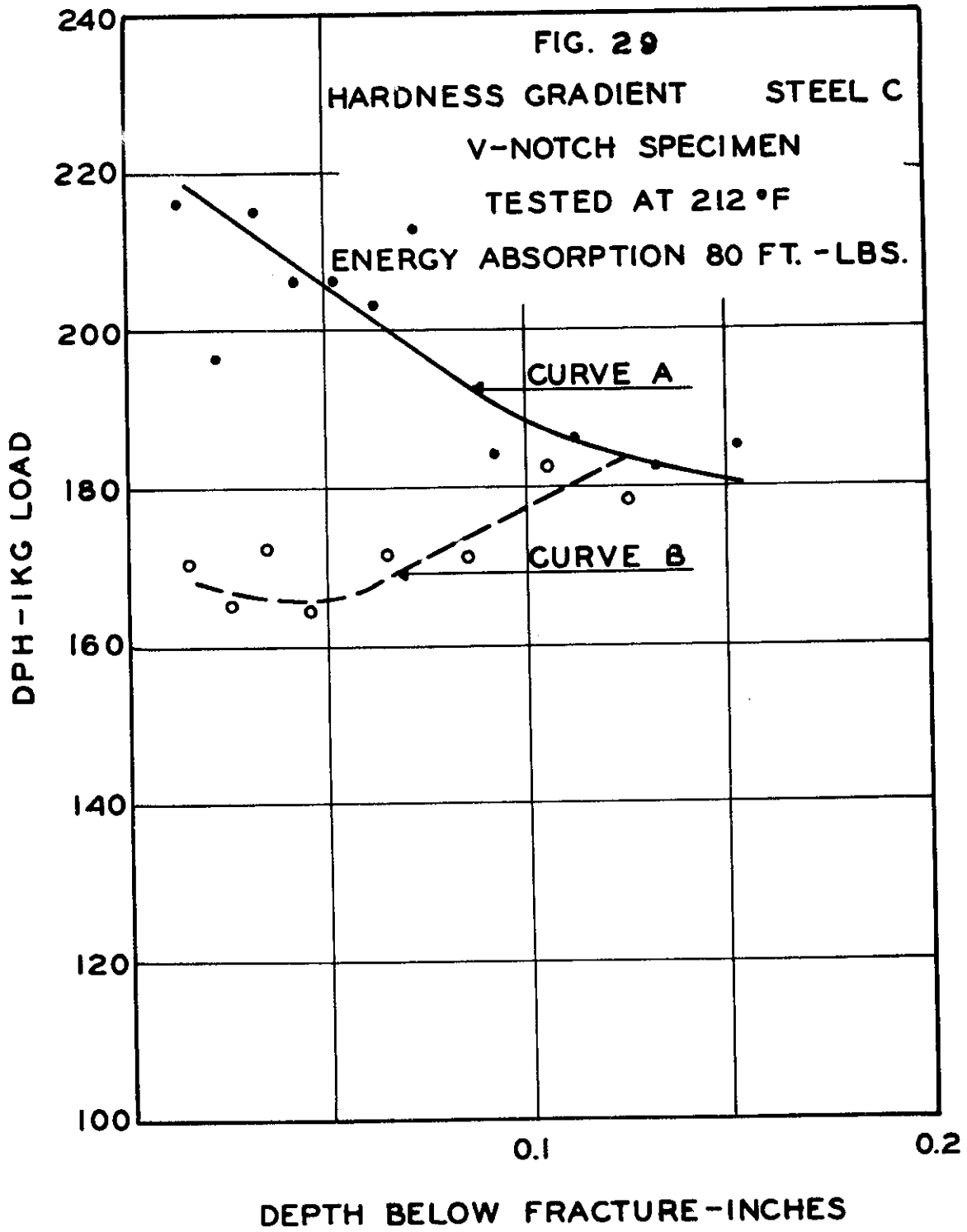
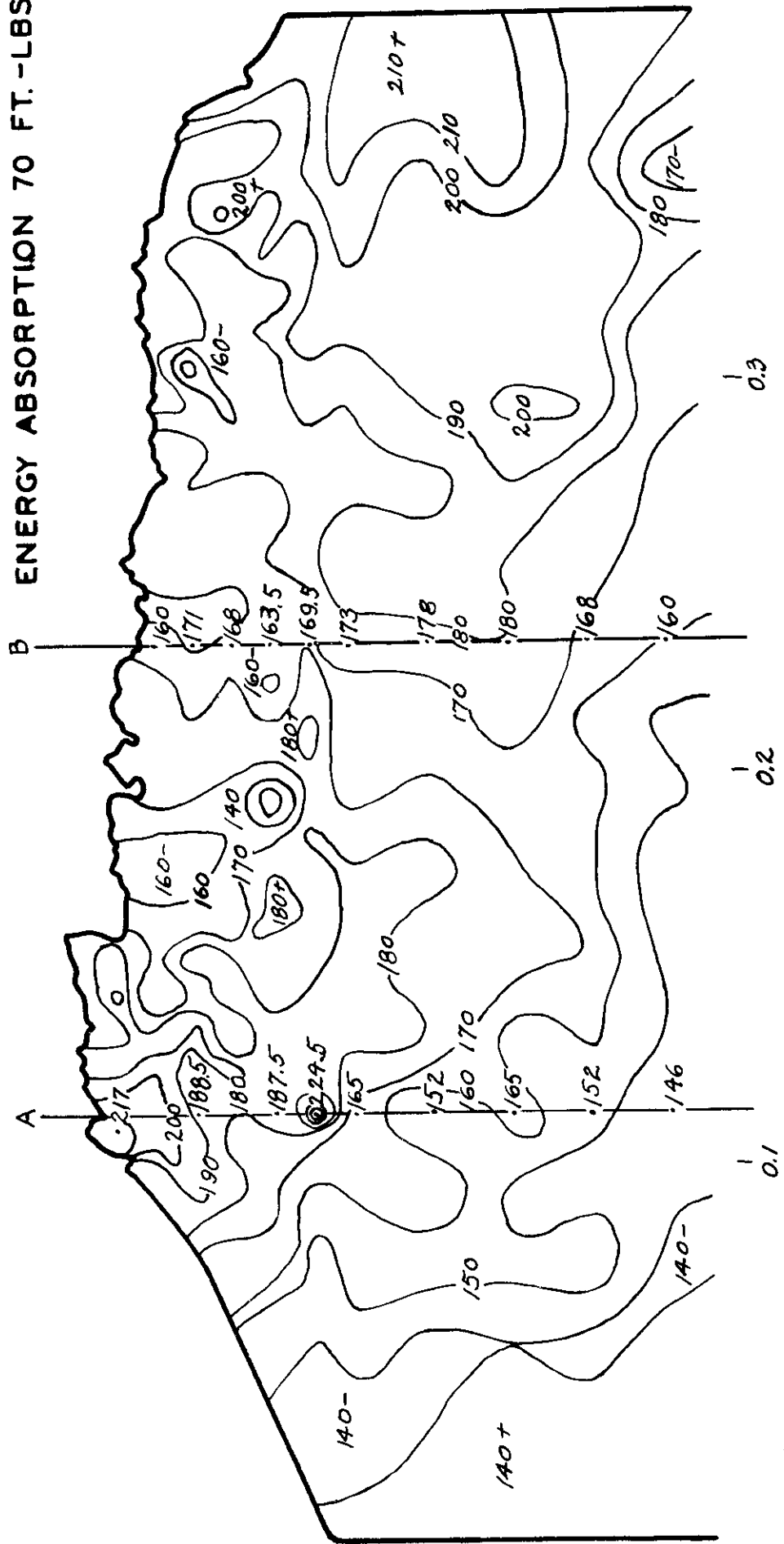
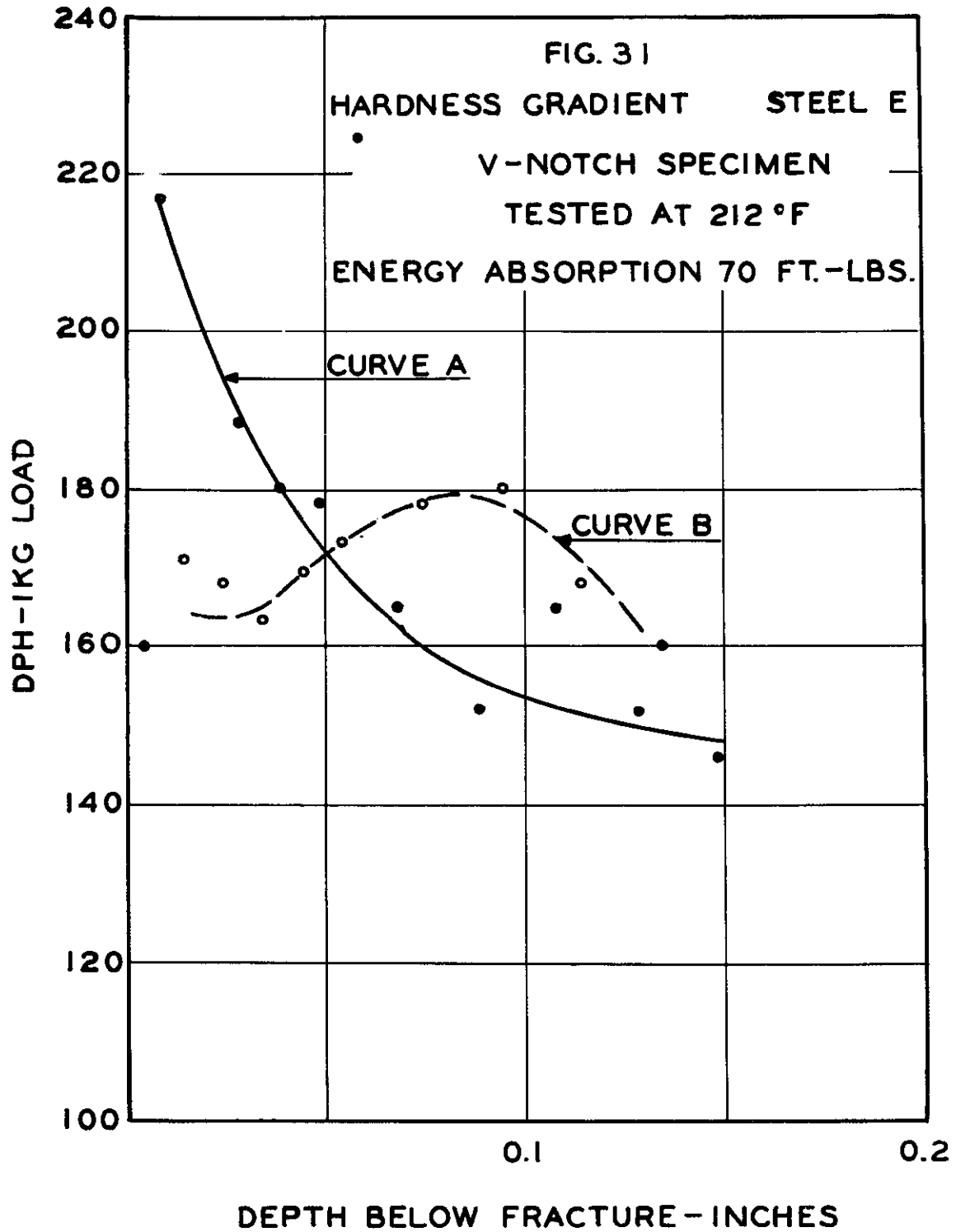


FIG. 30
 DPH CONTOURS STEEL E
 V-NOTCH SPECIMEN
 TESTED AT 212 °F.
 ENERGY ABSORPTION 70 FT.-LBS.





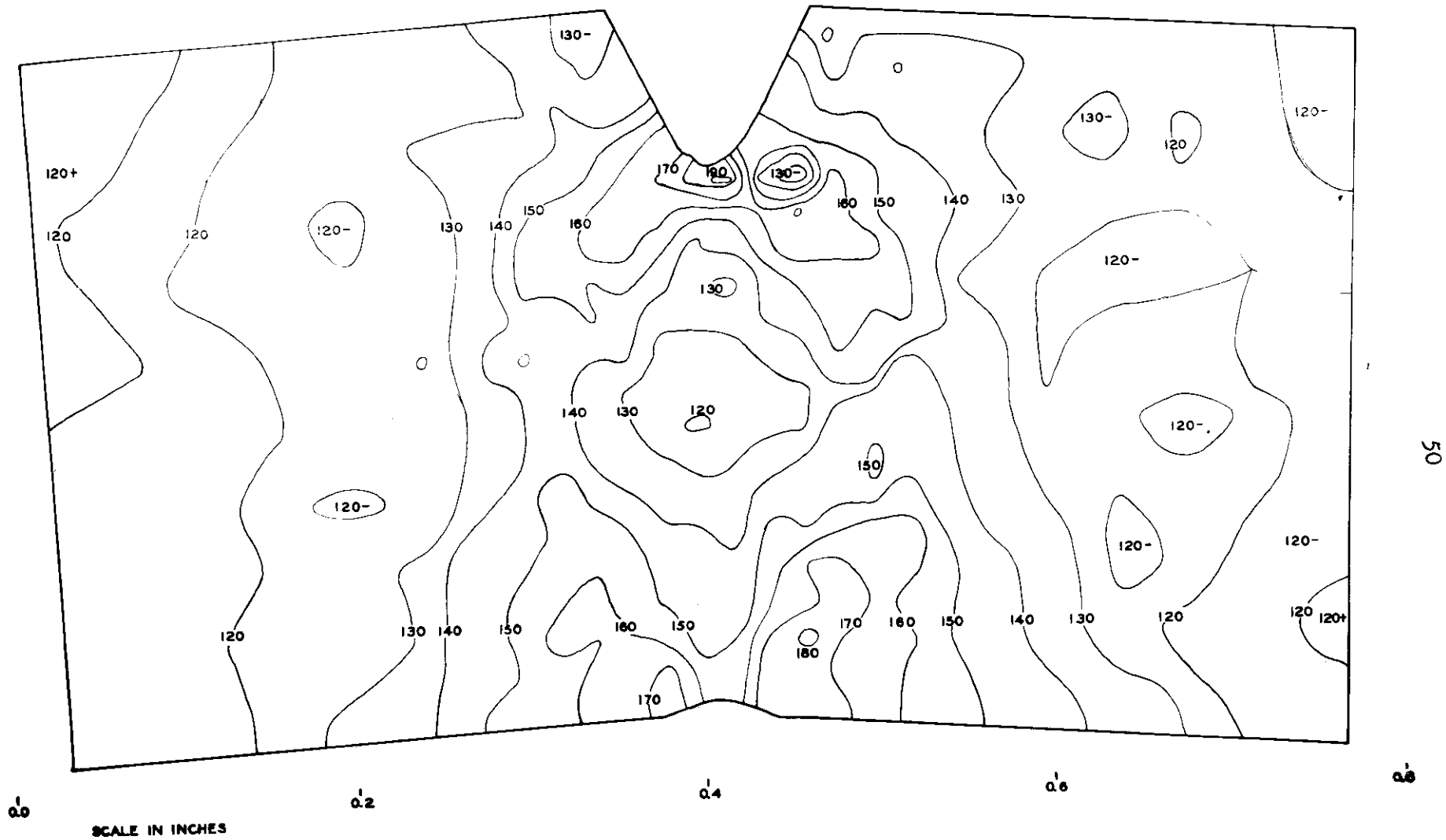
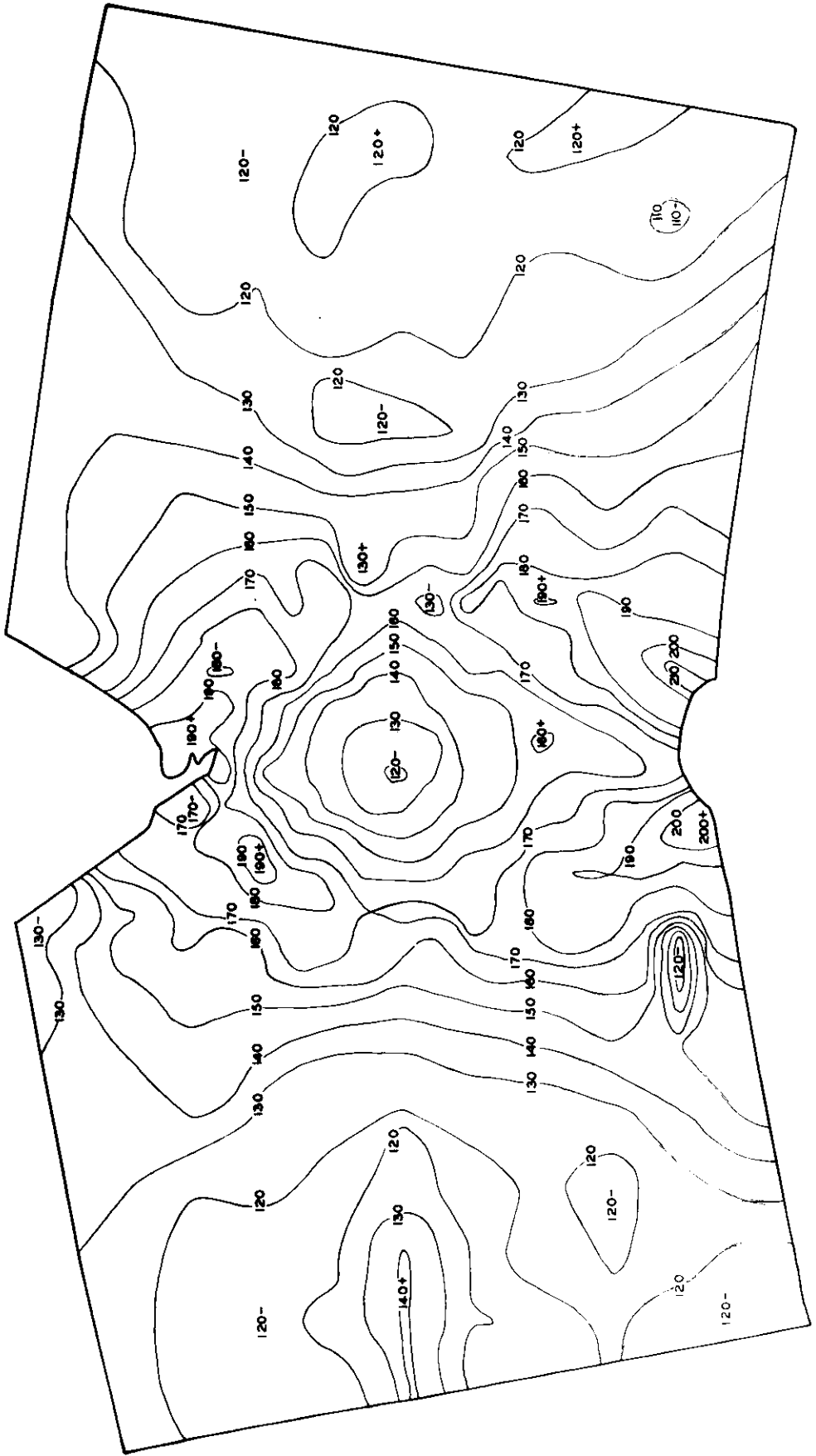


Fig. 32 - Hardness Contours - Steel C. Tested at 212°F; angle of bend = 9°, no crack formed. Kinetic Energy of Hammer = 13 ft. lbs.



0.0 0.2 0.4 0.6 0.8
SCALE IN INCHES

Fig. 33 - Hardness Contours - Steel C. Tested at 212°F, angle of bend = 22°, small crack formed. Kinetic Energy of Hammer = 34 ft. lbs.

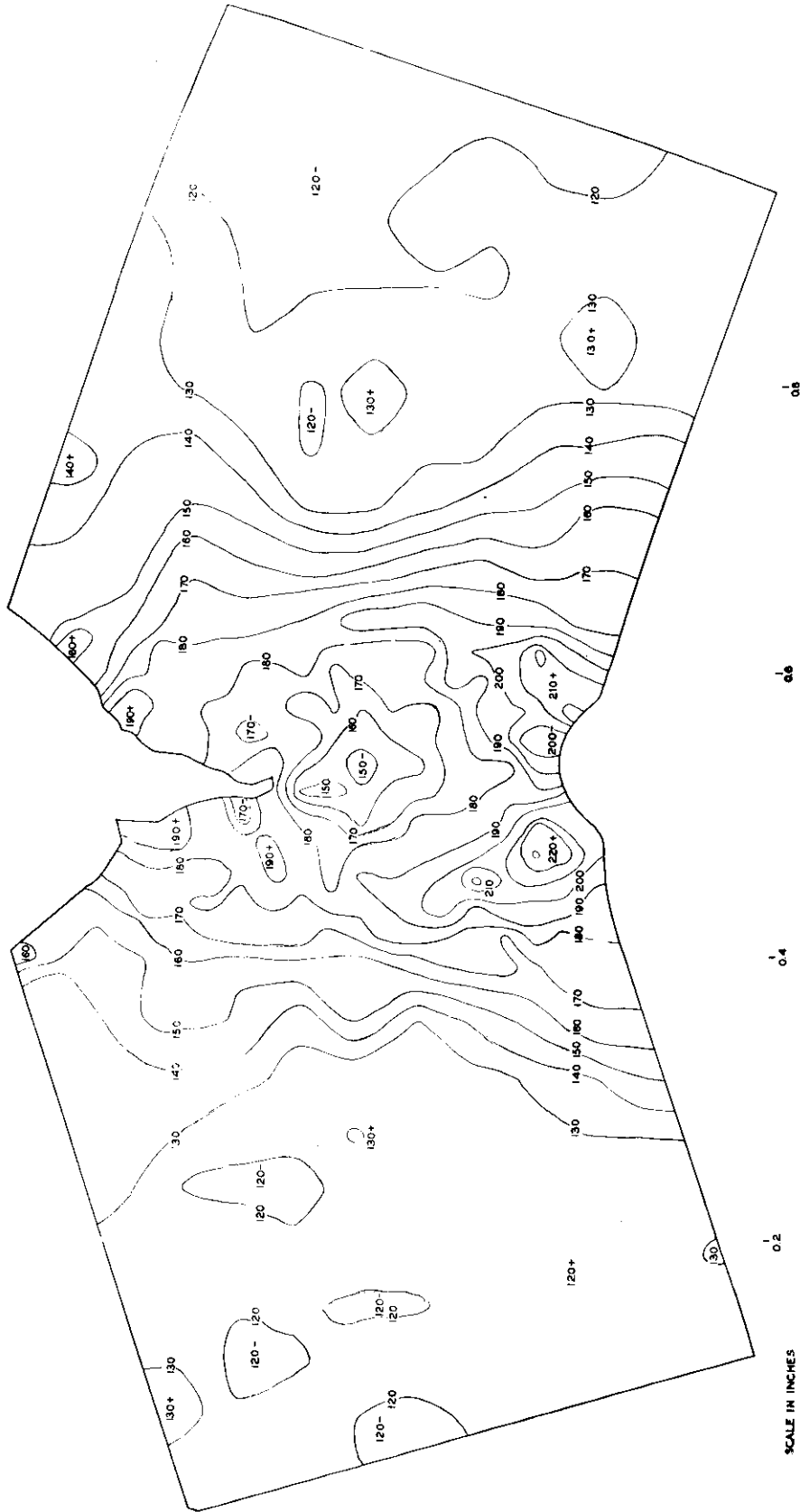


Fig. 34 - Hardness Contours - Steel C. Tested at 2120F, angle of bend = 38°, kinetic Energy of Hammer = 54 ft. lbs. crack through 1/3 of section.



FIG. 35 - Photograph of Plate C-3.

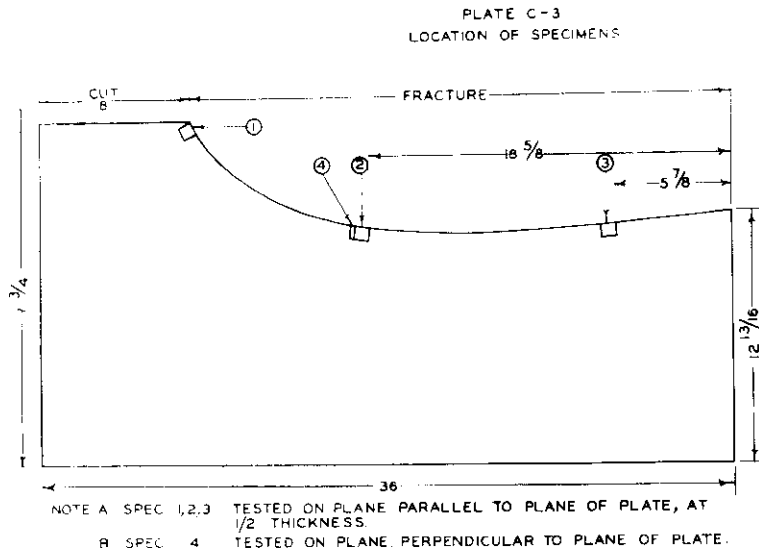


Fig. 36 - Line Drawing of Plate C-3.

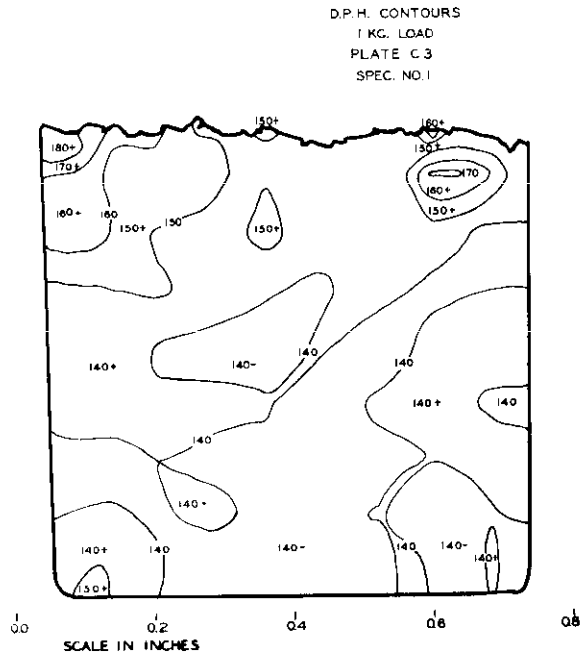


Fig. 37 - Hardness Contours - Specimen No. 1, Plate C-3.

D.P.H. CONTOURS
 1 KG. LOAD
 PLATE C3
 SPEC. NO.2

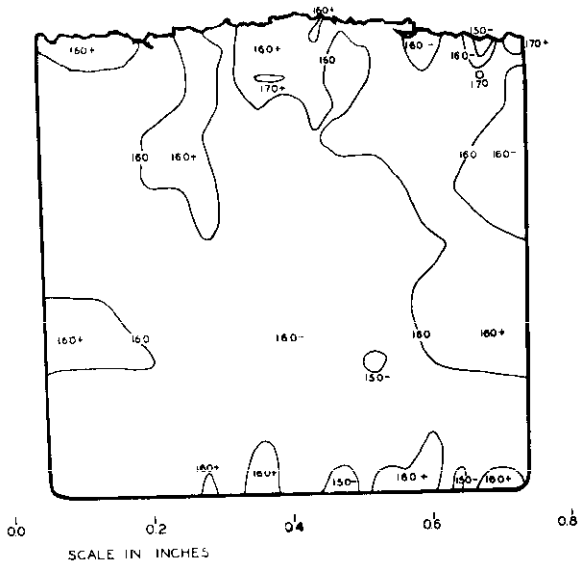


Fig. 38 - Hardness Contours
 Specimen No. 2, Plate C-3

D.P.H. CONTOURS
 1 KG. LOAD
 PLATE C3
 SPEC. NO.3

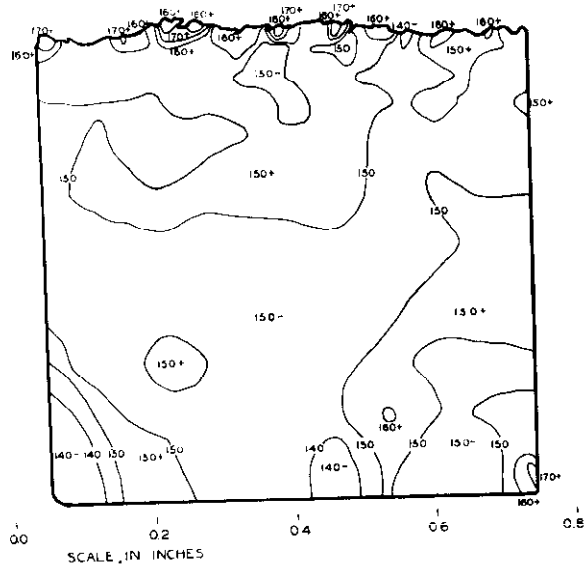


Fig. 39 - Hardness Contours
 Specimen No. 3, Plate C-3

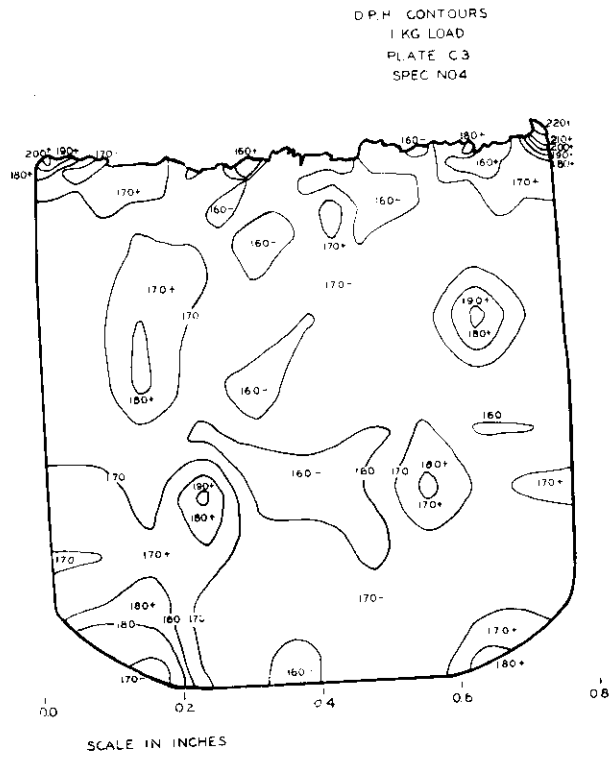


Fig. 40 - Hardness Contours
Specimen No. 4, Plate C-3



Fig. 41 - Photograph of Plate 22-1K.

PLATE 22-1K
LOCATION OF SPECIMENS

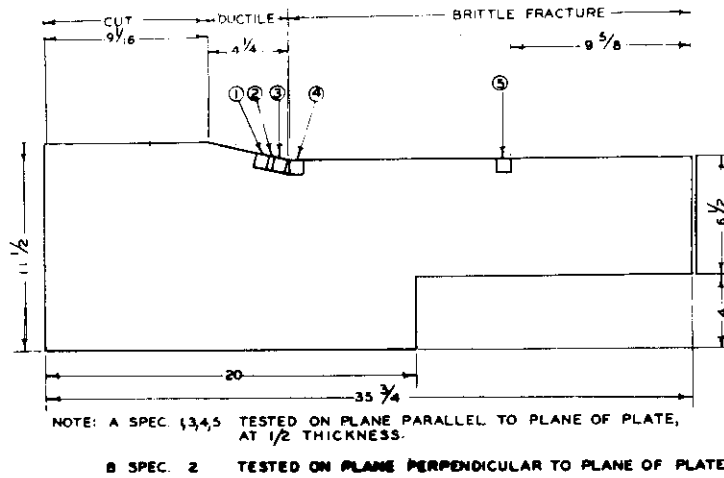


Fig. 42 - Line Drawing of Plate 22-1K.

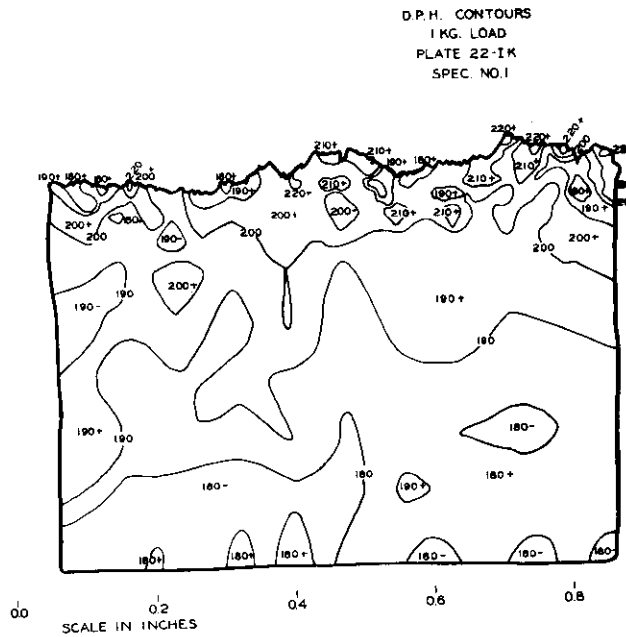
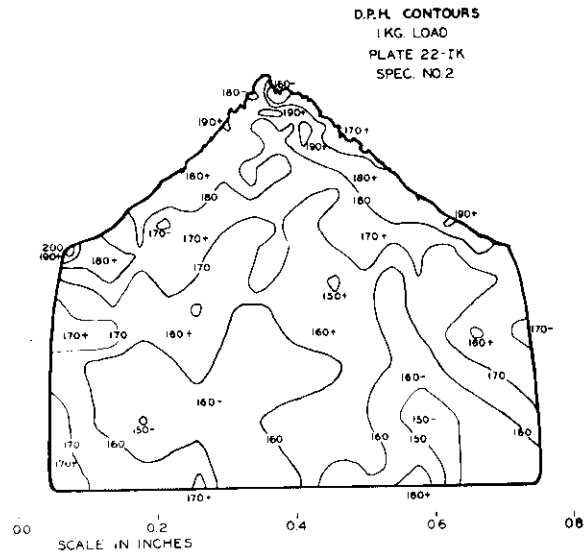
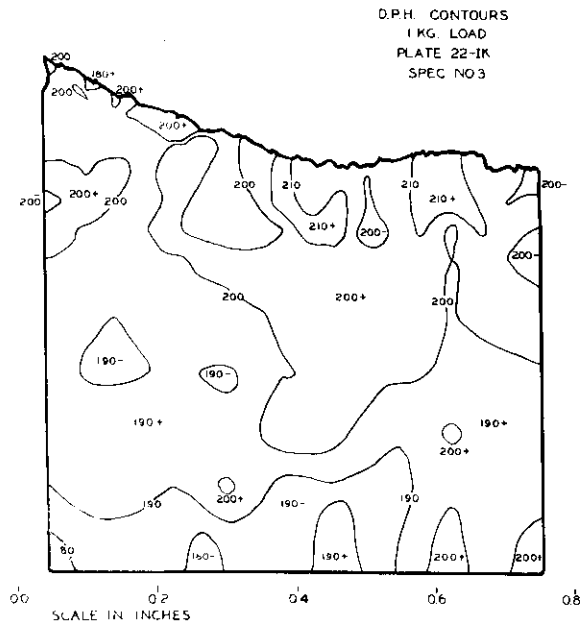


Fig. 43 - Hardness Contours
Specimen No. 1, Plate 22-1K.



**Fig. 44 - Hardness Contours
Specimen No. 2, Plate 22-1K.**



**Fig. 45 - Hardness Contours
Specimen No. 3, Plate 22-1K.**

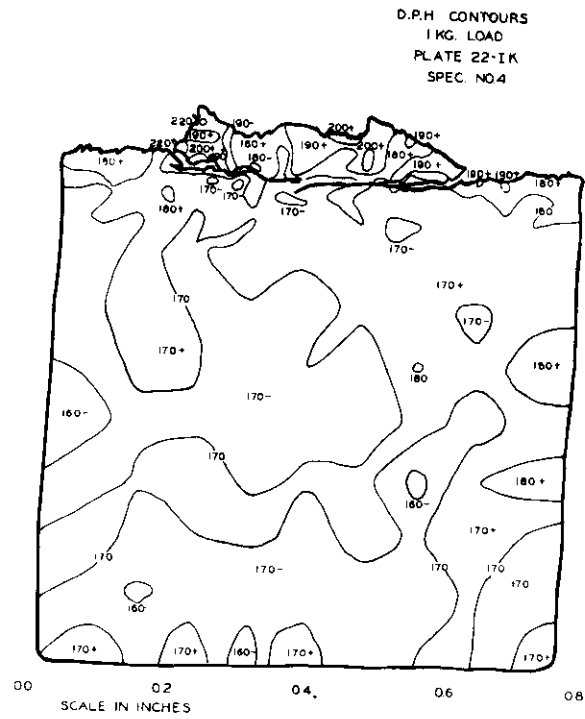


Fig. 46 - Hardness Contours
Specimen No. 4, Plate 22-1K.

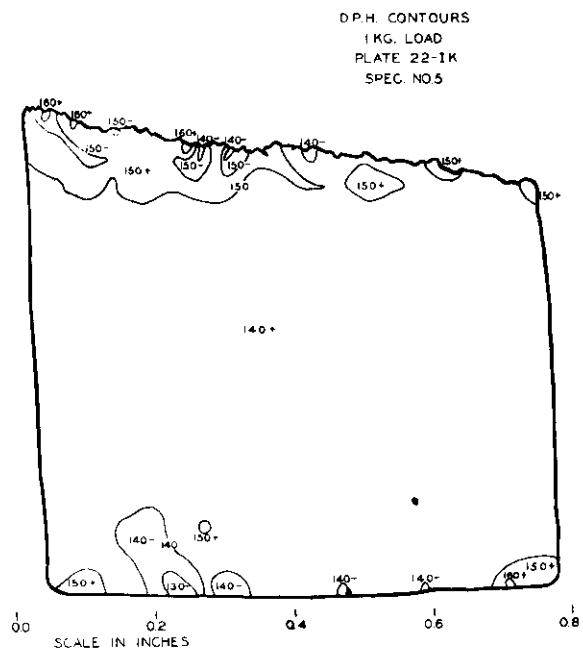


Fig. 47 - Hardness Contours
Specimen No. 5, Plate 22-1K.



Fig. 48 - Photograph of Plate N-1-A.

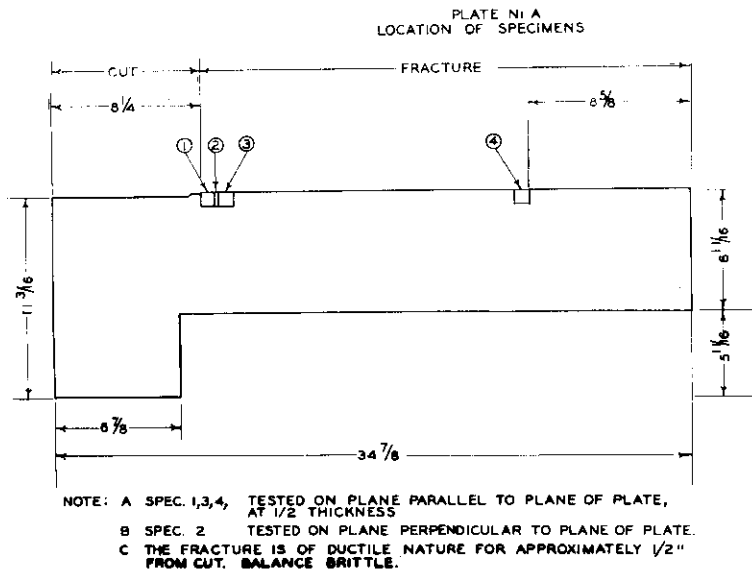


Fig. 49 - Line Drawing of Plate N-1-A.

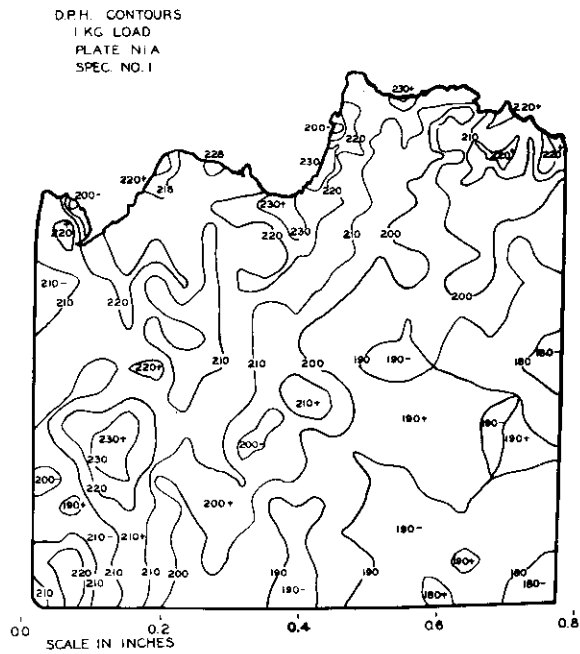
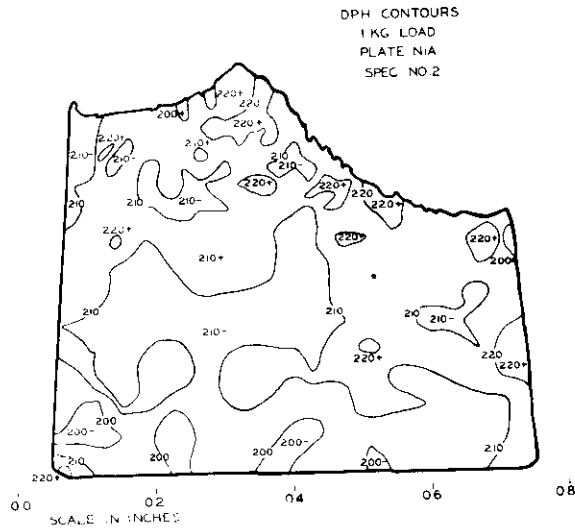
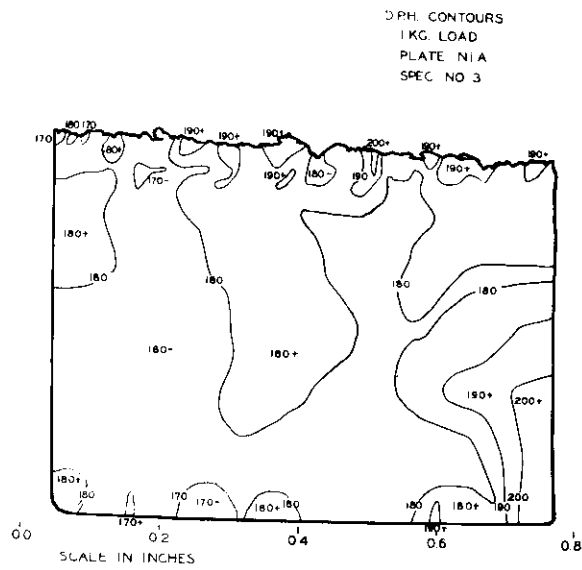


Fig. 50 - Hardness Contours
Specimen No. 1, Plate N-1-A



**Fig. 51 - Hardness Contours
Specimen No. 2, Plate N-1-A**



**Fig. 52 - Hardness Contours
Specimen No. 3, Plate N-1-A**

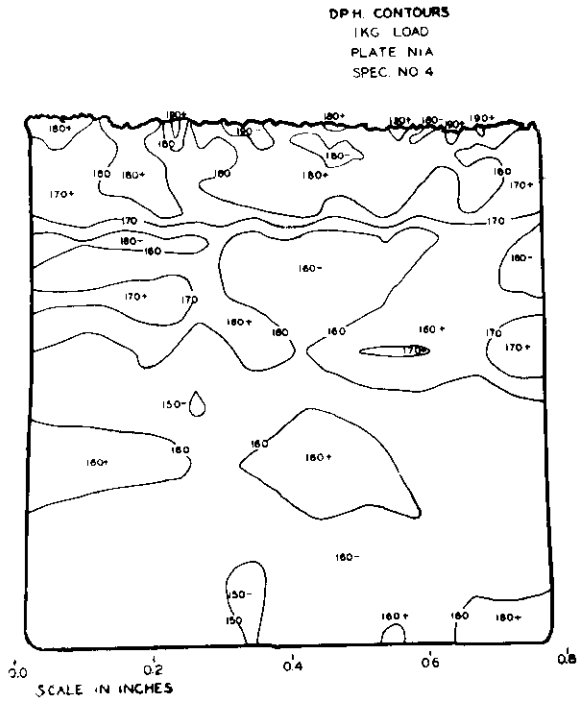
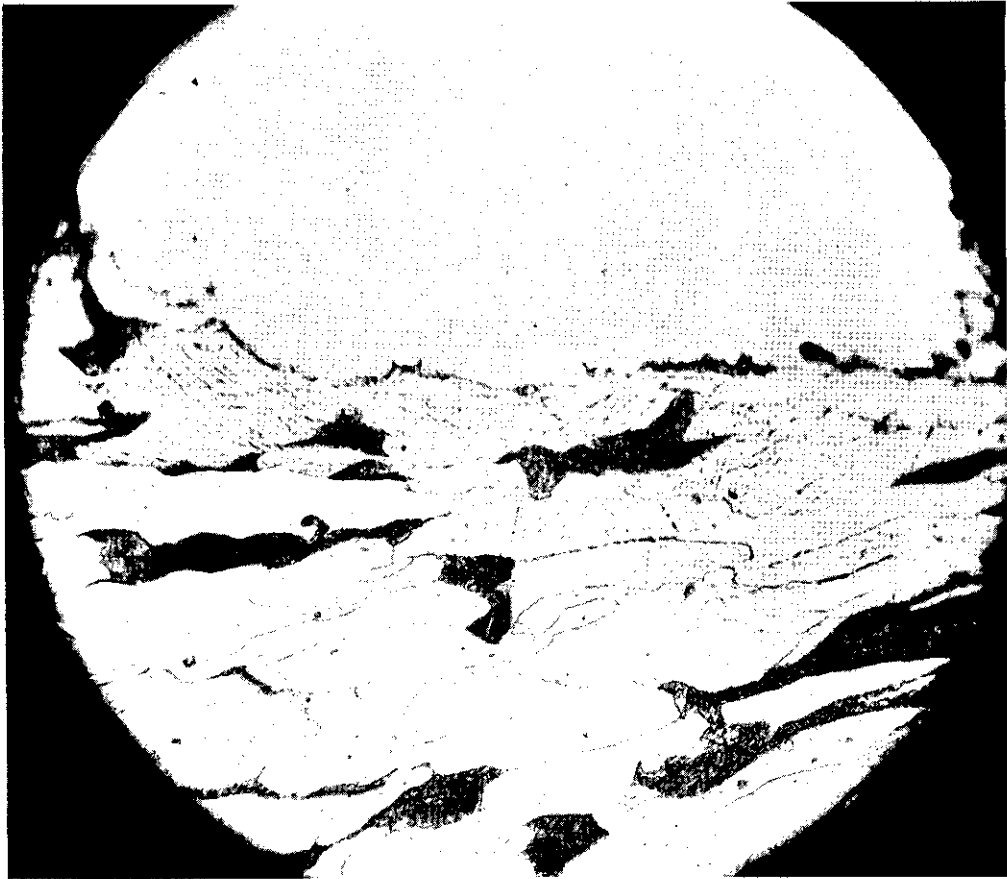


Fig. 53 - Hardness Contours
Specimen No. 4, Plate N-1-A



Fig. 54 - Deformation Twins in Steel C. Nital Etch x 600.



Fig, 55 - Strain Lines in Steel Dr. Nital Etch x 600.

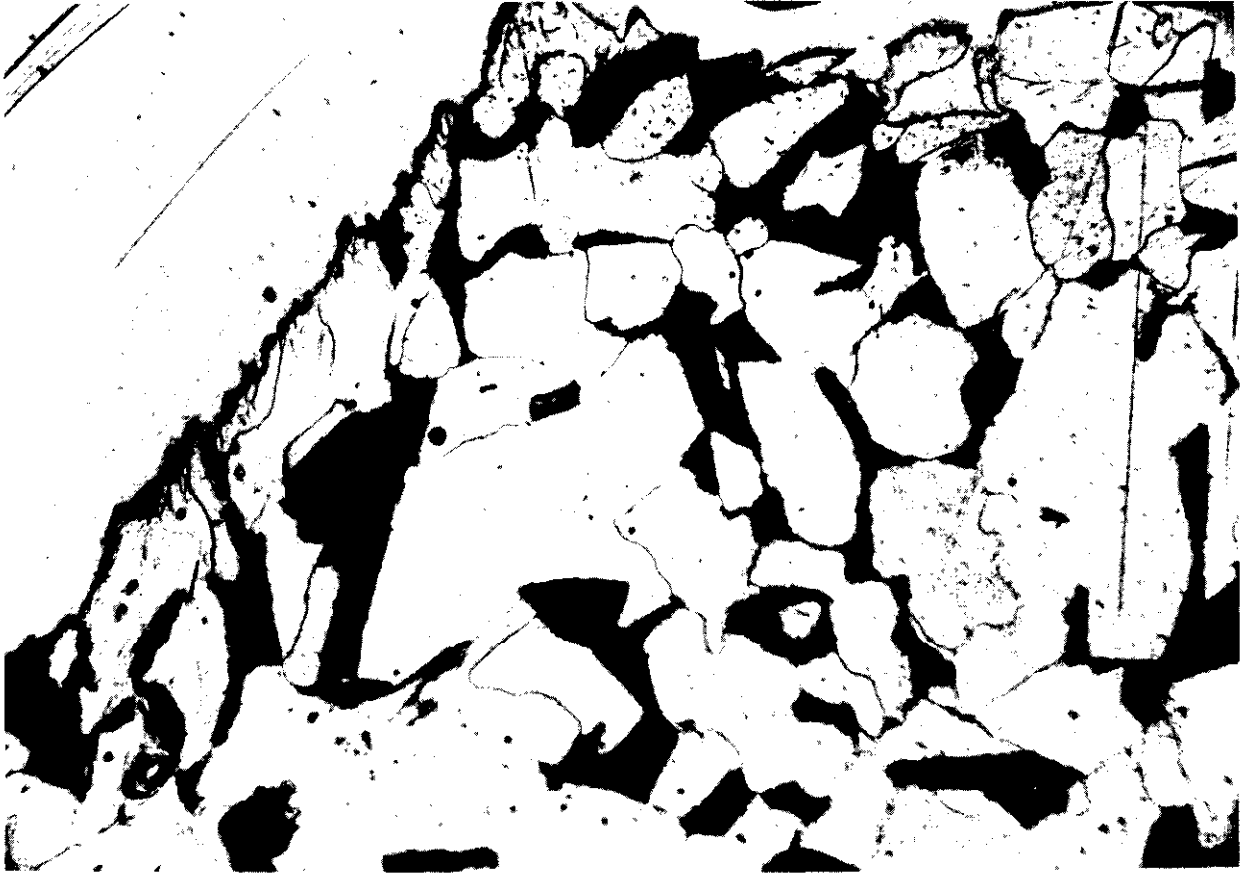


Fig. 56 - The Fracture for Specimen No. 4 Plate 22-1K showing Deformation Twins and Transition from Brittle to Ductile Failure. Nital Etch x 500

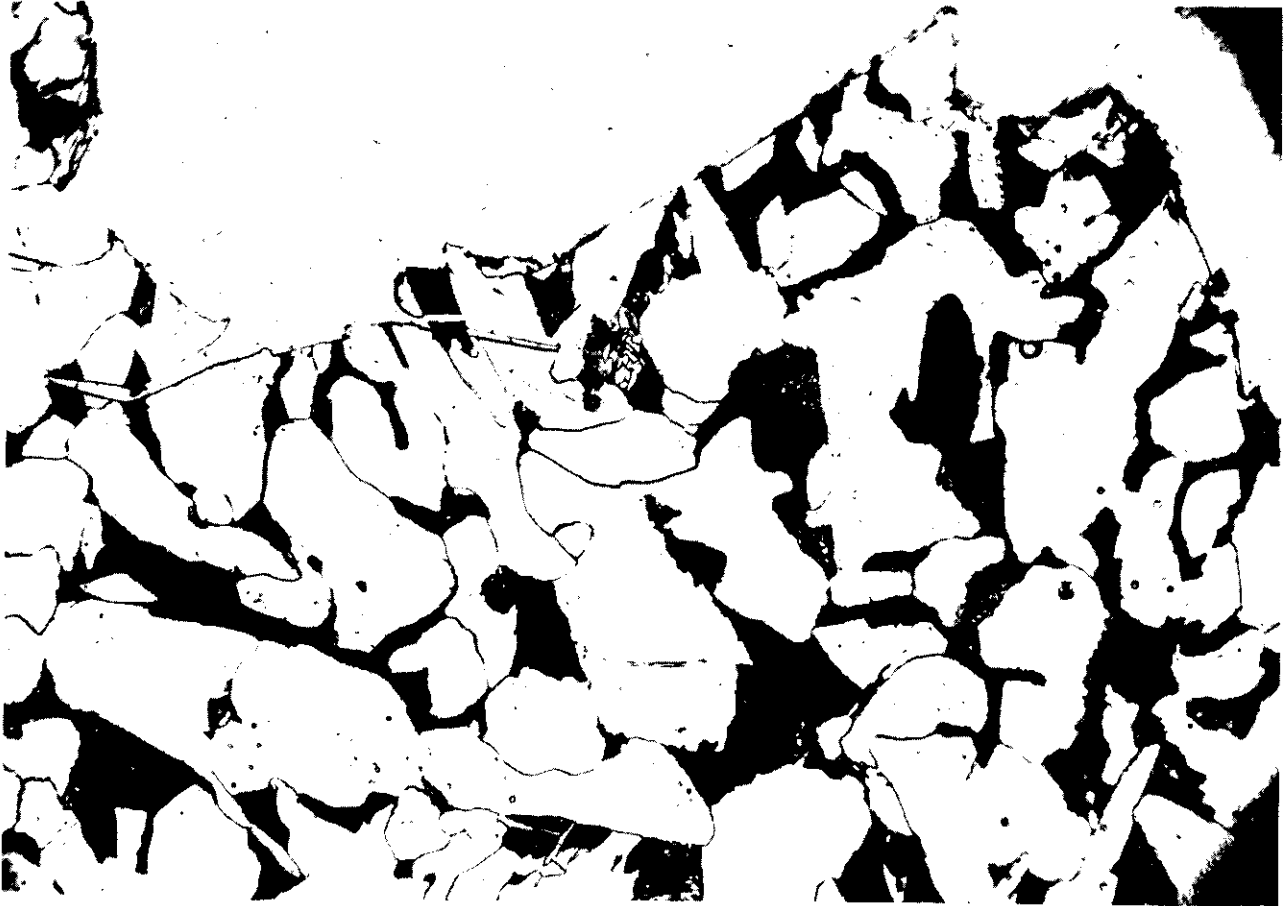


Fig. 57 - The Fracture for Specimen No. 5 Plate 22-1K showing Brittle Cracks of inter-and intra-granular types. Nital Etch x 500

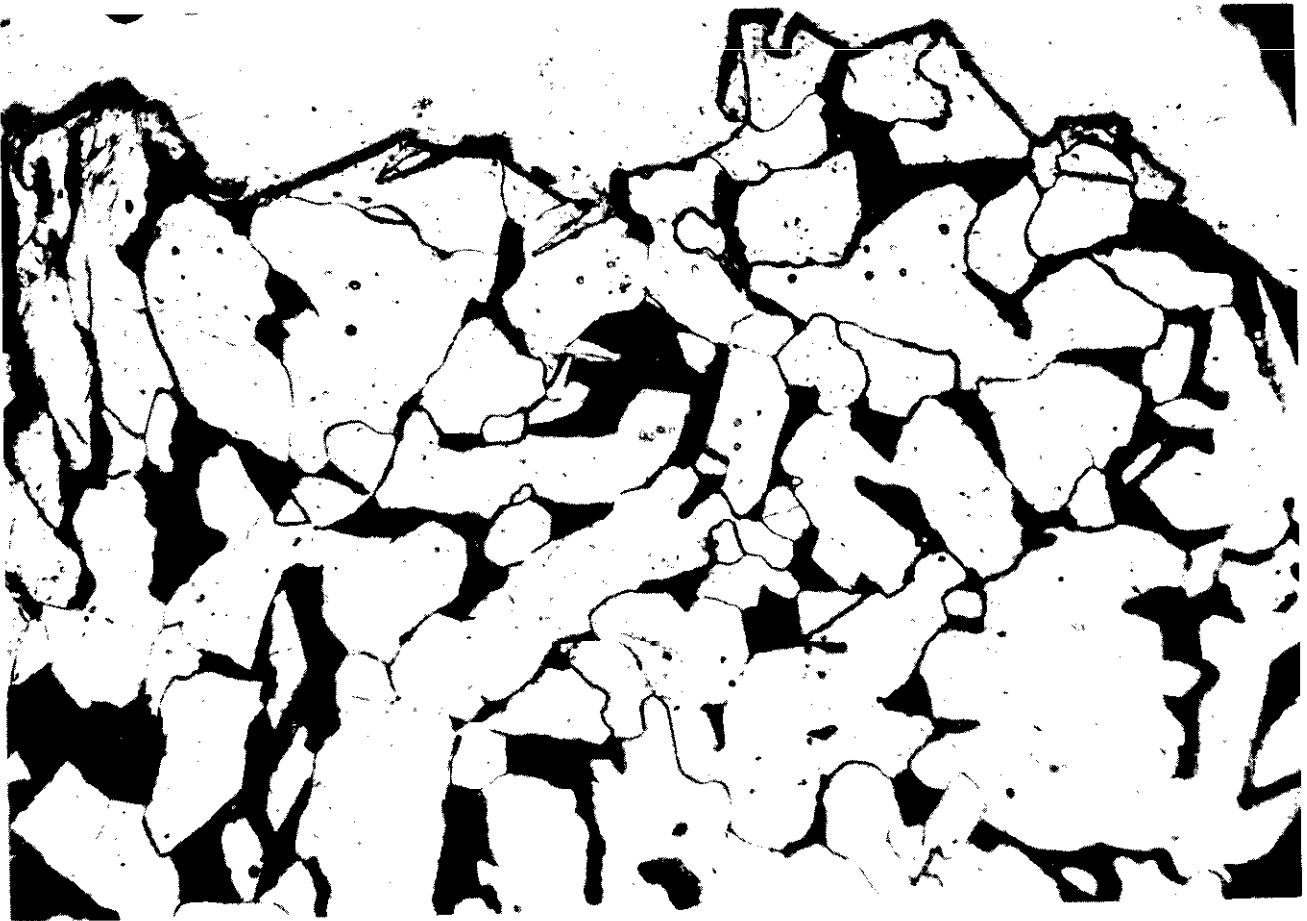


Fig. 58 - Another Region for Specimens No. 5 Plate 22-1K.
Nital Etch x 500



Fig. 59 - Character of the Fracture in Specimen No. 4
Plate 22-1K. Nital Etch x 500.